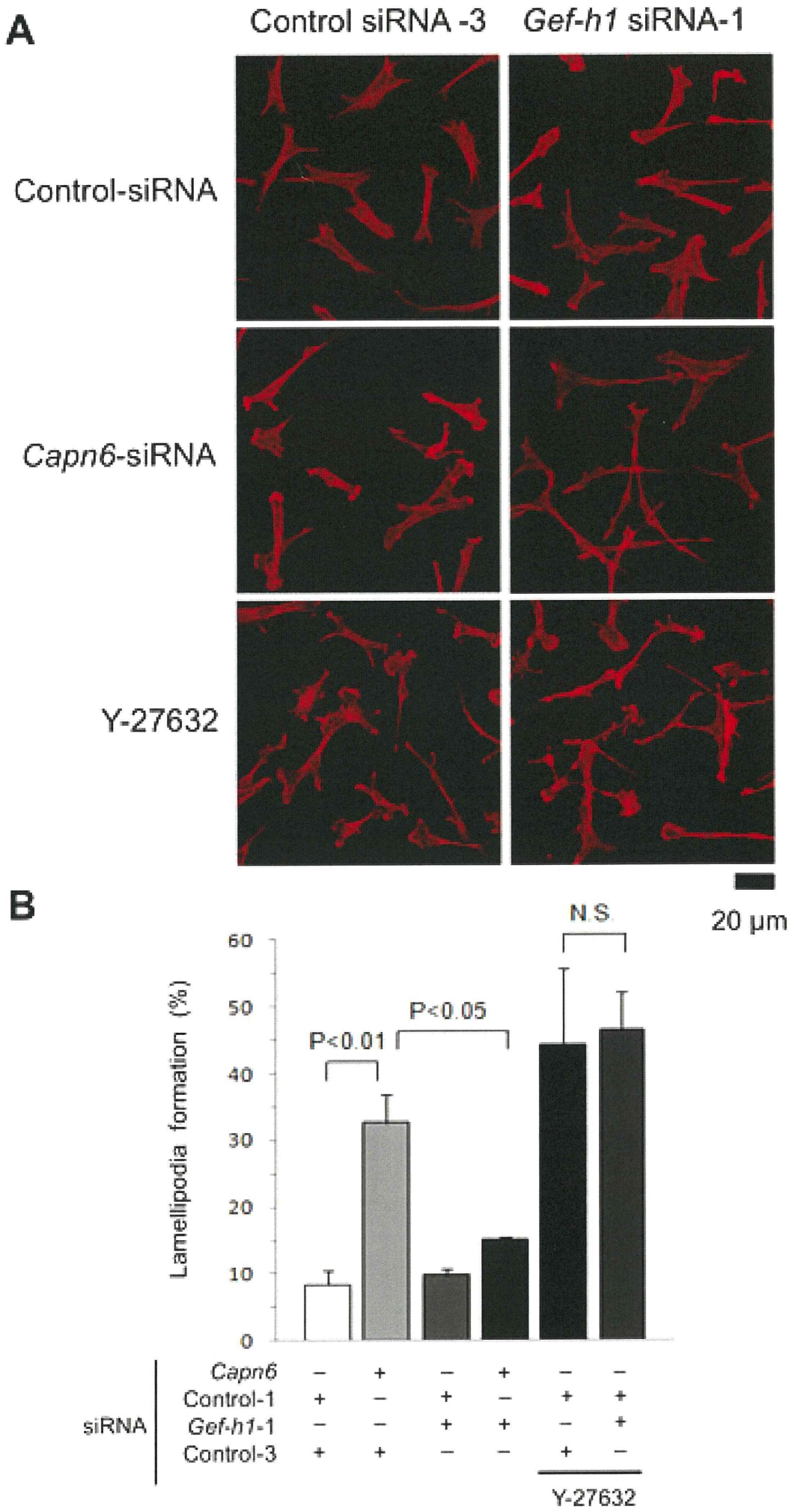
A
Control siRNA -3
Gef-h1 siRNA-1
Control-siRNA
Capn6-siRNA
Y-27632
20 μm
B
N.S
P<0.05
P<0.01
Lamellipodia formation (%)
60
50
40
30
20
10
0
Capn6 – + – + – –
siRNA Control-1 + – + – + +
Gef-h1-1 – – + + – +
Control-3 + + – – + –
Y-27632

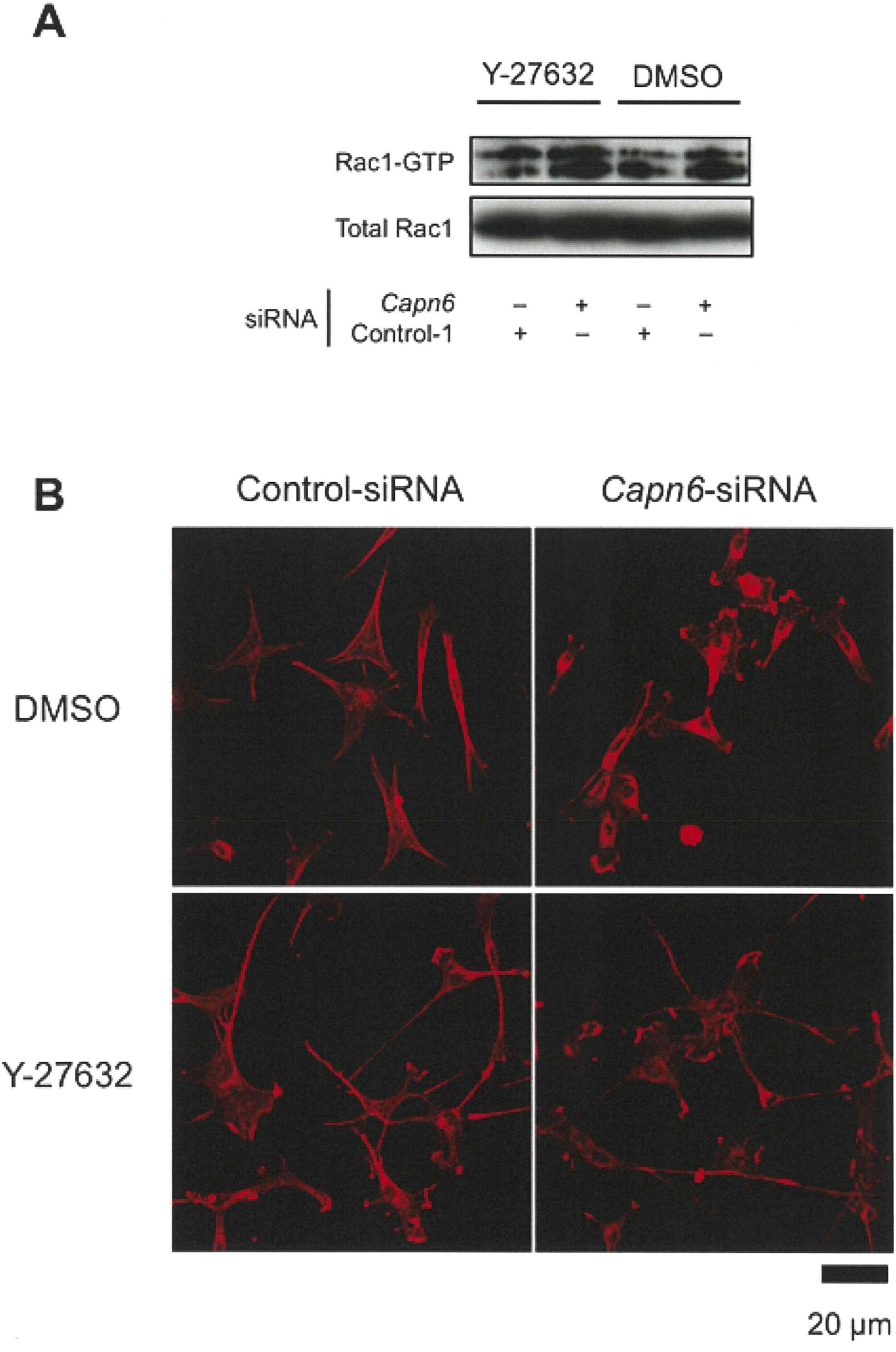
A
Y-27632
DMSO
Rac1-GTP
Total Rac1
siRNA
Capn6
Control-1
– + – +
+ – + –
B
Control-siRNA
Capn6-siRNA
DMSO
Y-27632
20 μm

Table S1. List of siRNAs used in this study

siRNA	Accession No.	Target nucleotides	Sequence
Capn6 siRNA -1	NM_007603	1518 to 1542	5'-GGUUCCGUCUUCACCAUCUGUAUAU-3'
Capn6 siRNA -2		1935 to 1959	5'-GGACCACUGACAUUCCUAUUAUCAU-3'
Rac1 siRNA	NM_009007	631 to 655	5'-GGCGAAAGAGAUCGGUGCUGUCAAA-3'
Gef-h1 siRNA -1	NM_008487	1085 to 1109	5'-CCCGGAACUUUGUCAUCCAUCGUUU-3'
Gef-h1 siRNA -2		3410 to 3434	5'-CCAUAAGUAUUGGAGAGCCUCUCCU-3'
RhoA siRNA	NM_016802	574 to 598	5'-GGGAAGCAGGUAGAGUUGGCUUUAU-3'

Control siRNA -1	Scrambled sequence of *Capn6* siRNA -1	5'-GGUUGCUUCCACUACGUCAUUCUAU-3'
Control siRNA -2	Scrambled sequence of *Rac1* siRNA	5'-GGCAGAACUAGGUGGUGUCCAGAAA-3'
Control siRNA -3	Scrambled sequence of *Gef-h1* siRNA -2	5'-CCAAUGAGGUUGAGACUCCUAUCCU-3'
Control siRNA-4	Scrambled sequence of *RhoA* siRNA	5'-GGGACGUGGAGAUUGCGGUUAAUAU-3'

Differentiation 81 (2011) 299–306

Contents lists available at ScienceDirect

Differentiation

journal homepage: www.elsevier.com/locate/diff

Tenascin C may regulate the recruitment of smooth muscle cells during coronary artery development

Katsumi Ando [a,1], Makiko Takahashi [b,1], Toshiyuki Yamagishi [b], Sachiko Miyagawa-Tomita [c], Kyoko Imanaka-Yoshida [d,e], Toshimichi Yoshida [d,e], Yuji Nakajima [b,*]

[a] Health Sciences Saitama Prefectural University
[b] Anatomy and Cell Biology Osaka City University Graduate School of Medicine
[c] Pediatric Cardiology Tokyo Women's Medical University
[d] Pathology and Matrix Biology Mie University Graduate School of Medicine
[e] Mie University Research Center for Matrix Biology

ARTICLE INFO

Article history:
Received 12 October 2010
Received in revised form
18 March 2011
Accepted 21 March 2011
Available online 16 April 2011

Keywords:
Tenascin C
Coronary vessel development
Smooth muscle cell
Avian heart

ABSTRACT

Tenascin C (TNC) is an extracellular glycoprotein that is thought to be involved in tissue remodeling during organogenesis and regeneration. Using avian embryonic hearts, we investigated the spatiotemporal expression patterns of TNC during the formation of the proximal coronary artery. Immunohistochemistry showed that TNC was deposited around the developing coronary stem and that TNC colocalized with vascular smooth muscle α-actin. A quail-chick chimera, in which a quail proepicardial organ (PEO) had been transplanted, showed that quail tissue-derived cells contributed to the establishment of the endothelial and mural cells of the proximal coronary artery, and the quail tissue-derived mural cells displayed TNC. Proepicardial cells cultured in TNC showed the myofibroblast/smooth muscle cell phenotype and neutralizing anti-TNC antibody suppressed the expression of smooth muscle markers. These observations suggest that TNC plays a role in the mural smooth muscle development of the nascent proximal coronary artery.

1. Introduction

Tenascin C (TNC) is an extracellular matrix glycoprotein that regulates various cellular events such as cellular differentiation, migration, survival, and proliferation (reviews, Jones and Jones, 2000; Imanaka-Yoshida et al., 2004; Tucker and Chiquet-Ehrismann, 2009; Midwood and Orend, 2009). It has been reported that TNC is expressed in regions where extensive tissue remodeling occurs during embryogenesis and organogenesis. The expression of TNC in adult tissue is very limited; however, its expression is significant in pathological lesions, such as cancer invasion and wound healing. In the adult heart, the expression of TNC is low but its expression is upregulated in lesion of myocardial infarction to recruit myofibroblasts (Imanaka-Yoshida et al., 2001a, 2001b; Tamaoki et al., 2005). During cardiovascular development, TNC is reported to be expressed in the precardiac mesoderm, valvuloseptal endocardial cushion tissue, subepicardial mesenchyme, and nascent great arteries (Hurle et al., 1990; Crossin and Hoffman, 1991; Sugi and Markwald, 1996; Imanaka-Yoshida et al., 2003; Zhang et al., 2006). Despite our knowledge of the spatiotemporal expression of TNC in the developing heart, the role of TNC is largely unknown, because TNC knockout mutant mice have only subtle phenotypic changes (Saga et al., 1992; Ishii et al., 2008; Gurevicius et al., 2009). However, recent reports have proposed that TNC plays multiple important roles during tissue repair (Midwood and Orend, 2009; Nishioka et al., 2010). For example, the involvement of TNC in angiogenesis has been suggested based on its expression being highly associated with angiogenesis in a wide range of pathological states, such as cancer (Jallo et al., 1997), diabetes (Castellon et al., 2002), and aortic aneurysms (Paik et al., 2004). In the heart, Ballard et al. (2006) demonstrated the essential role of TNC in postnatal angiogenesis.

During cardiogenesis, the coronary vascular system develops after the ventricular compact layer has thickened because nutrition and oxygen are unable to penetrate cardiac muscle by simple diffusion from the endocardium. Among vertebrates, mammals, birds, and reptiles have complete coronary systems, in which the coronary arteries originate from the aorta and lead to veins. In the remaining vertebrates, most amphibians have no coronary vessels and the presence of coronary vessels is variable in fish (Reese et al., 2002). Recently, the developmental mechanisms of coronary vasculogenesis have been reevaluated (Reese et al., 2002; Olivey et al., 2004;

* Corresponding author. Tel.: +81 6 6645 3705; fax: +81 6 6646 3603.
E-mail address: yuji@med.osaka-cu.ac.jp (Y. Nakajima).
[1] These authors contributed equally to this work (KA and MT).

0301-4681/$ - see front matter © 2011 International Society of Differentiation. Published by Elsevier Ltd. All rights reserved.
Join the International Society for Differentiation (www.isdifferentiation.org)
doi:10.1016/j.diff.2011.03.002

Mu et al., 2005; Ratajska et al., 2008). The key events of coronary system development include the generation of the proepicardial organ (PEO); the formation of the epicardium; the generation of the subepicardial mesenchyme; the formation, remodeling and migration of the final vascular plexus; and connection to the aortic sinuses (Mu et al., 2005). The PEO, a progenitor of the epicardium and coronary vessels that develops on the dorsal surface of the splanchnic mesoderm just ventral to the sinus venosus, migrates across the ventricular surface to establish the initial epithelial epicardium (Hiruma and Hirakow, 1989). The nascent epicardium seeds mesenchymal cells into the subepicardial extracellular space, where they differentiate into vascular endothelial, cardiac fibroblasts, and smooth muscle cells (Poelmann et al., 1993; Mikawa and Gourdie, 1996). Blood islands develop from the subepicardial mesenchyme, and they connect with each other to form sinusoidal communications on the surface of the heart (Hirakow 1983; Kattan et al., 2004). Thereafter, endothelial strands, which extend from the sinusoids surrounding the outflow tract, invade into the aortic sinuses. Later, the endothelial strands that have invaded into the facing sinuses (the right and left coronary sinuses) fuse to form a single coronary stem (Bogers et al., 1989; Waldo et al., 1990; Ando et al., 2004). After the coronary plexus and the aorta have become interconnected with each other, the coronary arteries recruit vascular smooth muscle cells and the adventitia for histogenesis of the coronary arterial wall in the proximal to distal direction (Vrancken Peters et al., 1997; Landerholm et al., 1999).

In the present study, using avian embryonic hearts, we investigated the immunohistochemical localization of TNC in developing coronary artery stems and examined whether TNC is capable of facilitating proepicardium-derived cells to differentiate into the myofibroblast/smooth muscle cell phenotype.

2. Materials and methods

2.1. Avian embryos

Quail and chick embryos were staged according to the Hamburger and Hamilton staging system (1992). Then, the staged embryos (at least 3 embryos per stage were prepared) were collected in phosphate-buffered saline (PBS) and fixed with 4% paraformaldehyde in PBS, which was injected into the ventricle using a fine glass needle. Their hearts were also fixed in 4% paraformaldehyde in PBS at 4 °C for 12 h. After being washed in PBS, the outflow tract regions were resected and embedded in paraffin. Serial 5 μm thick sections were cut, transferred to glass slides, and subjected to immunostaining.

2.2. Antibodies

The primary antibodies we used were as follows: rabbit polyclonal anti-TNC (Imanaka-Yoshida et al., 2001a, 2001b), monoclonal anti-TNC (clone 4F10, IBL, Gumma, Japan), anti-smooth muscle α-actin (SMA, clone 1A4, Sigma), anti-calponin (clone CP93, Sigma), anti-GAPDH (glyceraldehydes-3-phosphate dehydrogenase, CHEMICON), anti-quail cell (QCPN, Developmental Studies Hybridoma Bank), and anti-quail endothelial cell (QH1, Developmental Studies Hybridoma Bank). The following secondary antibodies were also used: TRITC-conjugated goat anti-mouse IgG2a, FITC-conjugated goat anti-mouse IgG1 (Southern Biotechnology), FITC-conjugated goat anti-rabbit IgG (MBL, Nagoya, Japan), and peroxidase conjugated goat anti-mouse IgG (MBL, Nagoya, Japan).

2.3. Indirect immunostaining

Indirect immunostaining was performed as described elsewhere (Ando et al., 2004; Tamaoki et al., 2005). After deparaffinization, the sections were blocked with 1% bovine serum albumin (BSA) in PBS and incubated with the primary antibody (mixture) followed by secondary antibody (mixture). Diaminobenzidine/H_2O_2 solution was used to demonstrate peroxidase conjugated antibody binding. The samples were observed under a conventional fluorescent or light microscope, and images were recorded with a cooled CCD camera.

To create superimposed images (Fig. 1), the outflow tract regions from ED5-8 quail hearts were embedded in paraffin, and serial cross sections were prepared. Each serially sectioned sample was placed on two sets of glass slides (one set for TNC staining and the other for QH1 and 1A4). Using TRI/3D-SRF-II (Ratoc System Engineering) and Photoshop (Adobe), the signals for each stain were converted into pseudo-color, and then the resulting images from 40 to 70 sections were superimposed onto each other. Whole-mount antibody staining was performed as described elsewhere (Kataoka et al., 1997; Metzger et al., 2008). The fixed hearts were incubated with monoclonal anti-TNC antibody (4F10), processed with TSA kit with HRP-goat anti-mouse IgG and Alexa Fluor546 tyramide (Molecular Probes), and subsequently incubated with FITC-conjugated anti-smooth muscle α actin. Then, the samples were observed under a laser confocal microscope (Zeiss).

The cultured epicardium was fixed with 4% paraformaldehyde/PBS for 1 h at RT, rinsed with PBS, and blocked with 1% BSA/PBS containing 0.1% triton X-100. Samples were then incubated with a primary antibody mixture (QH1/1A4 or CP93/1A4) at 4 °C overnight, rinsed with PBS and incubated with a secondary antibody mixture for 1 h at RT. The nuclei were then stained with DAPI for 20 min, rinsed with PBS, and mounted. Then, the samples were observed under a laser confocal microscope (Zeiss) or conventional fluorescent microscope (Olympus).

2.4. Epicardial culture experiment

ED6 quail or chick hearts were collected in PBS, and the epicardium was cultured according to a modified version of the method described by Compton et al. (2006). The hearts were placed ventral side down on 8-well chamber slides (Nunc), which had been coated with type I collagen (50 μg/ml, 12 h, Becton Dickinson), followed by coated with purified TNC (0–10 μg/ml, 12 h; Tamaoki et al., 2005), supplemented with serum free defined medium (75% DMEM, 25% McCoy's medium, containing 10^{-7} M dexamethasone and penicillin-streptomycin; Matsui et al., 2008). After 20 h incubation, the hearts were removed, and the remaining epicardial explants were cultured for up to 48–72 h. In neutralizing experiment, slides were coated with type I collagen and 5 μg/ml TNC, and epicardial explants were cultured in the medium supplemented with normal rabbit IgG (Sigma) or polyclonal rabbit anti-TNC neutralizing antibody (Tamaoki et al., 2005). Resultant cultures were observed under a phase contrast microscope to examine any phenotypic changes and then subjected to immunohistochemistry and Western blotting.

2.5. Western blotting

Six epicardium cultures were homogenized in SDS sample buffer (2 μl/explant) (62.5 mM Tris–HCl, 10% glycerol, 2% SDS, 5% 2-β mercaptoethanol, and 1 mM Na_3VO_4; pH6.8). After heat denaturation at 95 °C for 5 min, samples (approximately 5 μg of protein) were subjected to 10 or 12% SDS-polyacrylamide gel electrophoresis and then transferred onto Immobilon-P membranes (Millipore). After being blocked with 5% non-fat dry milk, the membranes were incubated with primary antibody for 2 h at room temperature. After being washed, they were incubated with horseradish peroxidase-conjugated secondary antibodies.

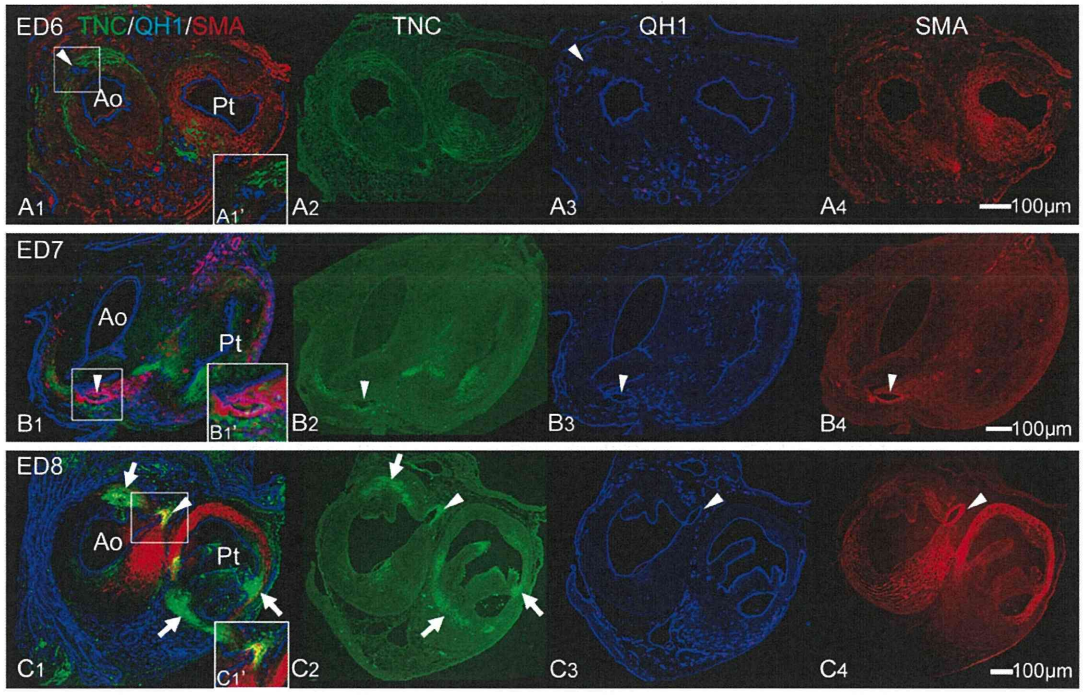

Fig. 1. Immunohistochemical localization of TNC, QH1, and SMA. *A1-4 (ED6)*: A QH1-positive endothelial strand, which is an anlage of the coronary stem, is invading the aortic wall (arrowheads). TNC was expressed around the outer wall of the aortic root but did not colocalize with the QH1-positive endothelial strand. A1' shows a high magnification of boxed area in A1. *B1-4 (ED7)*: At this stage, endothelial strands that penetrated the aortic sinus united to form a single coronary stem (arrowheads). TNC was deposited around the coronary stem, where SMA-positive mural cells accumulated (arrowheads). B1' shows a high magnification of boxed area in B1. *C1-4 (ED8)*: At this stage, the single coronary stem had fully developed, and both TNC and SMA were strongly expressed in the wall of the coronary artery (arrowheads). TNC was also deposited in the wall of the ascending aorta (Ao) and the pulmonary trunk (Pt), to which semilunar valves are connected (arrows). C1' shows a high magnification of boxed area in C1. Ao, ascending aorta; Pt, pulmonary trunk; QH1, quail endothelial marker; SMA, smooth muscle α-actin; TNC, tenascin C.

Immunoreactive bands were visualized using ECL detection reagent (Amersham).

2.6. Quall-chick PEO chimera

Quail-chick PEO chimeras were produced according to the method of Männer (1999). Stage 16–17 quail hearts were inspected to confirm that the PEO was not attached to the dorsal wall of the heart. Using an eggshell membrane, the quail PEO was isolated together with the sinus venosus and transplanted behind the chick heart. After an appropriate incubation period, the embryos were sacrificed, and their hearts were subjected to immunostaining for TNC and either QCPN or QH1.

3. Results

3.1. Immunohistochemical localization of tenascin C during coronary arterial stem development

We previously reported that during coronary arterial stem development in the quail embryonic heart, endothelial progenitor cells begin to invade into the aortic root at ED6, and the two-coronary system is completed at ED8 (Ando et al., 2004). To examine the spatiotemporal deposition of TNC during coronary artery stem development, we stained quail ED5-8 embryonic hearts with anti-TNC, QH1 (quail endothelial marker), and 1A4 (anti-smooth muscle α-actin, SMA) antibodies. At ED5, no QH1-positive endothelial strands (the anlagen of the coronary stem) penetrating the aortic wall were observed (not shown). At ED6-6.5, QH1-positive endothelial strands that penetrated the aortic wall were observed. TNC was distributed circumferentially in the wall of the aortic root; however, the TNC deposition did not coincide with the regions that the QH1-positive endothelial strands had penetrated (arrowheads in Figs. 1A and $3B_2$). At this stage, SMA was not detectable around the endothelial strands. At ED7, the endothelial strands penetrating the aortic sinus are unified and form a single coronary stem (Ando et al., 2004). At this stage, TNC was deposited around the coronary stem, where SMA-positive cells had accumulated (arrowheads in Fig. 1B). At ED8, the single orifice of the coronary artery had fully developed (arrowheads in Fig. 1C). TNC was deposited along the coronary arterial wall, in which SMA expression was extensive (arrowheads in Fig. 1C). TNC was also deposited in the aortic/pulmonary wall, to which semilunar valves were connected (arrows in Fig. 1C). Whole mount immunostaining of ED9 quail hearts showed that TNC was localized along the SMA-positive coronary artery (arrows in Fig. 2); and immunohistological tissue section showed that TNC was deposited around SMA-positive mural cells (arrowheads in Fig. 2). Our observations indicated that TNC was expressed at the developing proximal coronary artery, where SMA-positive cells, presumably prospective vascular smooth muscle cells of the tunica media, accumulated.

3.2. Quail-chick chimera experiments

It has been reported that both the endothelial and smooth muscle cells of coronary vessels originate from the PEO-derived subepicardial mesenchyme in avians (Mikawa and Gourdie, 1996; Männer, 1999), while the endothelial cells of coronary vessels are derived from the sinus venosus in mice (Red-Horse et al., 2010); thus, the origin of coronary endothelial cells is controversial. We next examined whether PEO-derived cells contribute to the proximal coronary artery. Quail-chick chimeras, in which quail

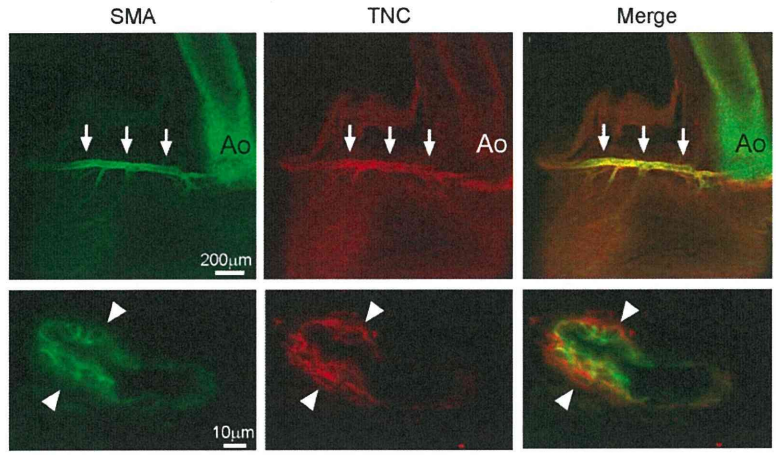

Fig. 2. A chick embryonic heart doubly stained for tenascin-C (TNC) and smooth muscle α-actin (SMA). Wholemount double immunostaining shows that TNC is localized along the SMA-positive coronary artery at the ED9 (arrows). Immunohistochemical staining of tissue section shows that the deposition of TNC is colocalized with SMA-positive mural cells in the developing coronary artery (arrowheads). Ao, ascending aorta.

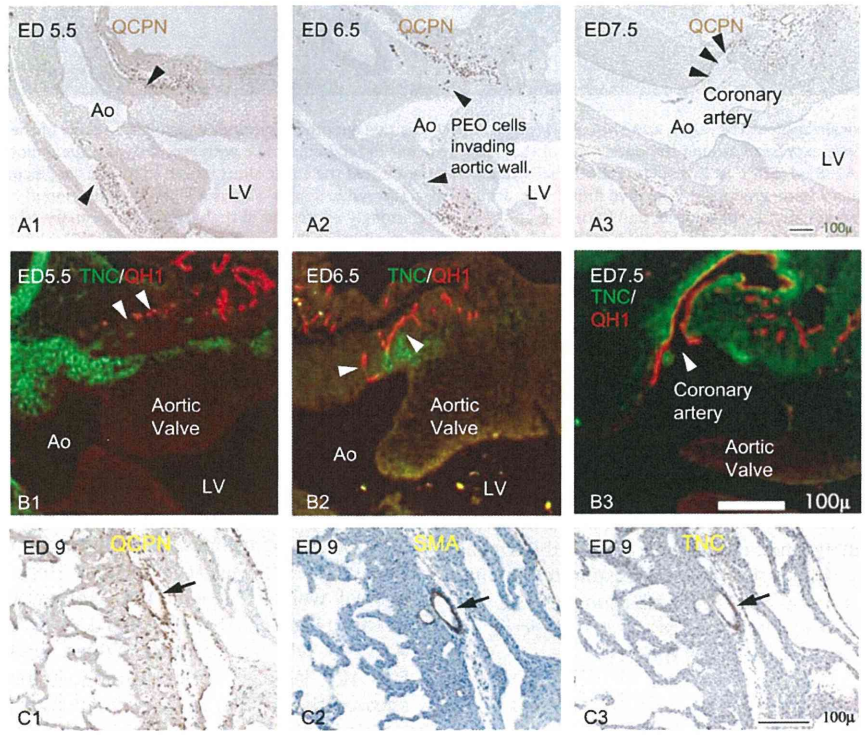

Fig. 3. PEO derived cells may develop into the endothelial and mural cells of the proximal coronary artery. Quail-chick chimeras, in which quail PEO were transplanted, were produced. After further incubation, the embryos were sacrificed, and the hearts were stained with antibodies for QCPN, QH1, 1A4, and TNC. *A1-3*: In chimeric chick hearts, QCPN-positive cells were found around the base of the ascending aorta (Ao) at ED 5.5 (arrowheads in A1), in the aortic wall at ED 6.5 (arrowheads in A2), and later in the endothelial lining of the proximal coronary artery (arrowheads in A3). *B1-3*: Transplanted PEO-derived QH1-positive endothelial cells are found around the aortic root at ED 5.5 (arrowheads in B1), in the aortic wall at ED 6.5 (arrowheads in B2), and in the endothelial lining of the coronary stem at ED7.5 (arrowheads in B3). From ED5.5-6.5, TNC was deposited in the aortic root but its association with QH1-positive cells was unclear (B1, 2). After the single coronary artery had fully developed, TNC was deposited subjacent to the QH1-positive endothelial cells (B3). *C1-3*: In the developing proximal coronary artery, both the QCPN and SMA-positive mural cells expressed TNC (arrows in C1-3). Ao, ascending aorta; ED, embryonic day; LV, left ventricle; QCPN, quail nuclear marker; QH1, quail endothelial marker; SMA, smooth muscle α-actin; TNC, tenascin C.

PEO had been transplanted, were produced and stained with QCPN (a quail nuclear marker), QH1 (a quail endothelial marker), 1A4, and anti-TNC. In chick embryonic hearts, in which quail PEO had been transplanted, QCPN-positive quail cells were found around the root of the ascending aorta (brown dots indicated by arrowheads in Fig. $3A_1$) and later in the aortic wall (arrowheads in Fig. $3A_2$). At ED 7.5, when the single coronary orifice had fully formed, both endothelial and subendothelial cells expressed the quail marker QCPN (arrowheads in Fig. $3A_3$). In the chimeric heart, TNC deposition (green in Fig. 3B) was observed in the root of the aorta, but no clear colocalization with QH1-positive quail PEO-derived endothelial progenitors was observed (red, Figs. $3B_1$, B_2). After the completion of the single coronary stem, strong anti-TNC staining became detectable subjacent to the QH1-positive

coronary endothelial cells (Fig. 3B$_3$). Immunostaining for TNC, QCPN and SMA in daughter sections prepared from chimeric chick heart showed that TNC, QCPN and SMA were deposited in the mural cells of the proximal coronary artery, suggesting PEO-derived mural cells (presumably nascent smooth muscle cells) express TNC (arrows in Fig. 3C). Similarly prepared sections, which were doubly stained with anti-SMA and QCPN, showed that SMA was expressed in QCPN-positive mural cells (CA in Supplemental Fig. 1). Observations suggest that PEO-derived cells contribute to the development/differentiation of both the endothelial and smooth muscle cells of the proximal coronary arteries and that TNC expression is closely associated with the recruitment of PEO-derived mural cells.

3.3. Cultured epicardial cells with TNC show SMC characteristics

We next examined whether TNC facilitates the differentiation of epicardial cells into smooth muscle cells in culture. The nascent epicardia from ED6 hearts were cultured on chamber slides with or without purified TNC. After 72 h, the cultures were examined for phenotypic changes under a phase-contrast microscope (Fig. 4A). In the epicardia cultured on slides coated with TNC, the cultures showed a whirl-like appearance, which was consisting of spindle-shaped cells and similar to hill-and-valley morphology without thick multilayer (Figs. 4A$_2$ and A$_3$). On the other hand, the epicardial cells cultured without TNC showed a typical cobblestone appearance (Figs. 4A$_1$ and A$_3$). The resulting cultures were subjected to immunological detections for SMA expression. Western blot analysis showed that the amount of SMA was predominant in cells cultured with TNC in a dose dependent manner (Fig. 4B). Immunostaining showed that the epicardial cells cultured without TNC showed tight cell-cell contact and that many cells expressed the quail endothelial marker QH1 (Fig. 4C). On the other hand, the cells cultured with TNC were separated and expressed SMA (Fig. 4D). We next examined whether anti-TNC neutralizing antibody (Tamaoki et al., 2005) was capable of inhibiting the expression of smooth muscle markers. The epicardia from ED6 chick heart were cultured on TNC-coated slide supplemented with medium containing anti-TNC antibody for 48 h, and resultant cultures were subjected to immunological detections for smooth muscle markers (Fig. 5). As shown in Fig. 5A, epicardial cells cultured in control medium (containing normal rabbit IgG) expressed SMA and calponin (Fig. 5A). On the other hand, the epicardial cells cultured with anti-TNC antibody showed a weak staining for SMA and calponin (Fig. 5B). Western blot showed that the expression of SMA was reduced in cultures treated with ant-TNC antibody (Fig. 5C). These results suggest that TNC is capable of facilitating the differentiation of epicardial cells into myofibroblast/smooth muscle cells in culture. We further examined whether TNC is able to induce the migration of epicardium-derived mesenchymal cells into a TNC-rich environment. A transwell migration assay was performed, and the results showed that there was no significant difference in the number of cells that migrated across the wall between the control and TNC-rich cultures (Supplemental Table 1).

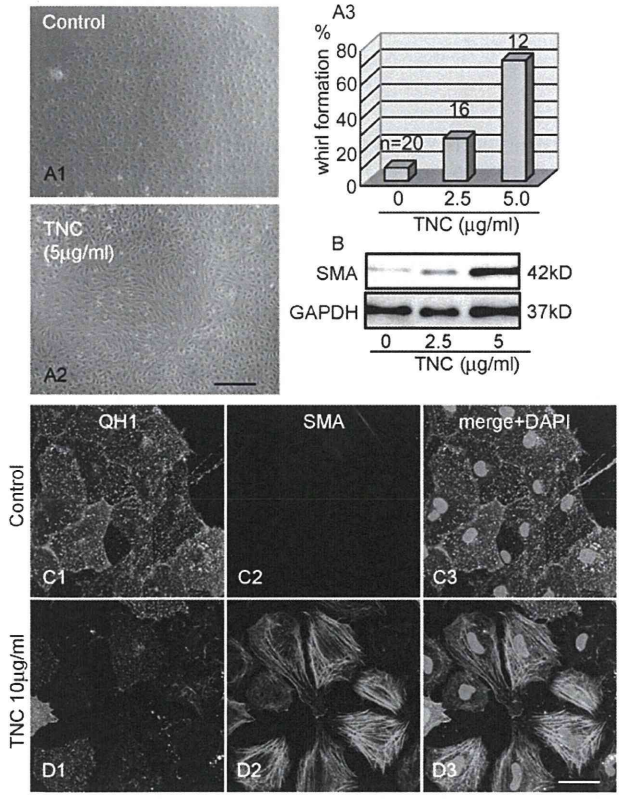

Fig. 4. The epicardium cultured in TNC showed smooth muscle cell characteristics. The nascent epicardia from ED6 quail hearts were cultured with or without TNC. After 72 h, the cells cultured in TNC showed a whirl-like appearance consisting of spindle-shaped cells (A2, 3), while the control cultures showed a typical cobble stone appearance (A1, 3). Western blotting showed that SMA was predominantly expressed in the cells cultured in TNC (B). Immunostaining showed that the epicardial cells cultured without TNC showed tight cell-cell contact and expressed the quail endothelial marker QH1 (C). On the other hand, the cells cultured in the TNC were separated and expressed SMA (D). A1 and 2, phase-contrast microscopic images; DAPI, nuclear staining; GAPDH, glyceraldehyde-3-phosphate dehydrogenase; QH1, quail endothelial marker; SMA, smooth muscle α-actin; TNC, tenascin C. Bar, 250 μm (A); 10 μm (C and D).

4. Discussion

4.1. Possible role of TNC in vascular development

During vascular development, vessels are initially established as endothelial tubes, which are subsequently supported by mural cells, such as the pericytes of capillary vessels and the vascular smooth muscle cells of the tunica media. In the present study, we showed that the deposition of extracellular TNC was closely associated with the onset of the formation of the thick SMA-positive vascular wall of the proximal coronary stem. When the single coronary stem has fully developed, both SMA and TNC are present in its mural cell layer. Furthermore, TNC altered the phenotype of the cultured proepicardium so that it resembled that of myofibroblasts or smooth muscle cells. These findings suggest that TNC may play a significant role in smooth muscle cell recruitment into the developing coronary arterial wall. Recently, our group has reported that TNC and PDGF collaboratively potentiate migration and proliferation of smooth muscle cell through crosstalk signal between integrin $\alpha v\beta 3$ and PDGFRβ by increased SRC recruitment and FAK activation (Ishigaki et al. 2010). During coronary development, endothelially-secreted PDGFB and mesenchymally expressed PDGFRβ interact with each other to recruit smooth muscle cells into the nascent tunica media (Hellström et al., 1999; Van Den Akker et al., 2005). Taking together, it is suggested that TNC may facilitate smooth muscle cell differentiation/organization in the wall of the coronary artery by modulating PDGF/PDGFRβ signaling via certain integrins.

Our immunohistochemistry showed that the deposition of TNC colocalized with the expression of SMA in mural cells; however, TNC did not coincide with endothelial progenitor cells. This observation suggested that TNC facilitates the recruitment of

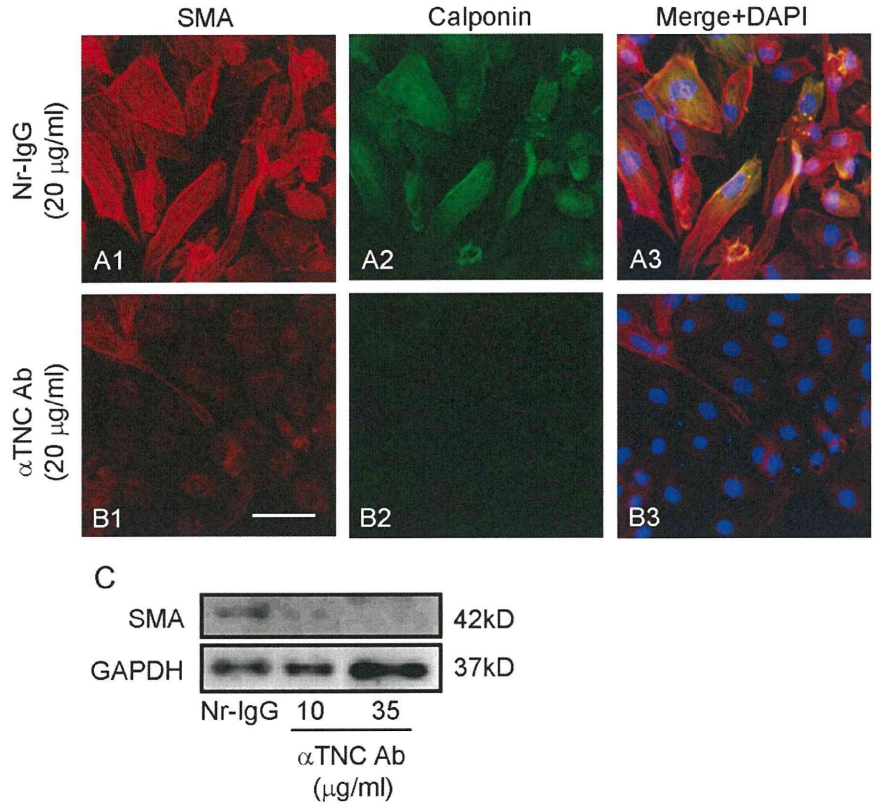

Fig. 5. Anti-TNC antibody suppressed the expression of SMA in cultured epicardium. The epicardia from ED6 chick hearts were cultured on TNC-coated slide with medium containing anti-TNC neutralizing antibody. After 48 h, the cells were subjected to immunological detection for SMA and calponin. Immunostaining showed that the epicardial cells cultured in control medium (containing normal rabbit IgG) expressed SMA and calponin (A). On the other hand, epicardial cells cultured with anti-TNC antibody showed that a weak staining for SMA and calponin (B). Western blot showed that the expression of SMA was reduced in cultures treated with anti-TNC antibody (C). αTNC Ab, anti-tenascin C neutralizing antibody; DAPI, nuclear staining; GAPDH, glyceraldehyde-3-phosphate dehydrogenase; Nr-IgG, normal rabbit IgG; SMA, smooth muscle α-actin. Bar, 40 μm. Note that exposure times for SMA calponin were 125 ms and 1 s, respectively.

SMC progenitors during vascular development, but not guidance for invasion/migration of endothelial progenitors. In myocardial lesions in the adult, TNC is thought to induce SMA-positive myofibroblast accumulation during wound healing and tissue remodeling (Imanaka-Yoshida et al., 2001a, 2001b; Tamaoki et al., 2005). Cardiac fibroblasts obtained from TNC-null mutant mice showed lower migratory activity and reduced expression of SMA than wild type cells in culture, and the addition of purified TNC to TNC-null cardiac fibroblasts reversed both the migration and expression of SMA, suggesting that TNC facilitates the migration and differentiation of myofibroblast cells (Tamaoki et al., 2005). TNC is also expressed in neoplastic lesion and plays a significant role in angiogenesis during cancer invasion (Midwood and Orend, 2009). In glioblastoma multiforme, TNC is highly up-regulated at the invasive edge in association with vascular sprout (Zagzag et al., 2002). *In vivo* and *in vitro* experiments suggest that TNC in matrix micro-environment in cancer may potentiate angiogenesis in tumor development (Zagzag et al., 2002; Tanaka et al., 2004). These observations suggest that the role of TNC in coronary artery development may be different from that in tumor angiogenesis. It is also suggested that TNC is capable of playing a distinct role during vasculogenesis/angiogenesis in a context-dependent manner.

Extracellular TNC binds to several integrins at FN-III domains to mediate intracellular signaling (Jones and Jones, 2000). Therefore, other extracellular matrices that possess FN-III domains, such as vitronectin, tenascin-X, and -R, might interact with certain integrins and maintain integrin-mediated intracellular signaling during smooth muscle cell growth. This might be one of the reasons why TNC-null mutant mice do not show lethal abnormalities during embryogenesis (Saga et al., 1992). The spatiotemporal expression patterns of TNC in regions where smooth muscle cell/myofibroblast differentiation occurs suggest that TNC plays a role in the recruitment of smooth muscle cells during vascular development including development of the coronary artery.

4.2. Origin of the cells forming the proximal coronary artery

It has been reported that the proepicardium gives rise to cells that contribute to coronary endothelial and smooth muscle cells in chicks (Mikawa and Gourdie, 1996; Männer, 1999), while recent experiments in apelin-nlac-Z knock-in mice have shown that the coronary arteries are not derived from the proepicardium but rather from endothelial sprouts of the sinus venosus (Red-Horse et al., 2010). Quail-chick chimera experiments showed that both endothelial and mural cells possessed quail markers, suggesting that these cells are derived from transplanted quail tissue (Fig. 3; Männer, 1999). However, in chimera experiment quail PEO was transplanted together with the sinus venosus; thus, we could not rule out the hypothesis that coronary endothelial cells originate from the sinus venosus in avians. The quail PEO is reported to consist of two distinct cell types, which include a superficial mesothelial epithelium and an internal mesenchymal core (Nahirney et al., 2003). The internal mesenchymal core, which is adjacent to endothelial lining of the sinus venosus, possesses endothelial marker QH1 (Ishii et al., 2009). Therefore, it may be possible that the QH1-positive mesenchymal

cells in the PEO are derived from the endothelial cells of the sinus venosus. Further experiments should be necessary to elucidate the origin of the coronary endothelial cells in avians.

It has been reported that *PDGFRβ*$^{-/-}$ hearts failed to form coronary arterial tunica media, but that epicardial-specific deletion of *PDGFβ* resulted in a reduced number of coronary vascular smooth muscle cells, suggesting that two sources of coronary vascular smooth muscle cells exist (Mellgren et al., 2008). Neural crest-derived cells are found in the walls of the proximal coronary arteries in Wnt1-Cre/R26R mice (Jiang et al., 2000), but mesenchymal cells in the anterior heart field do not give rise to coronary vessels (Verzi et al., 2005). Therefore, neural crest cells might contribute to the formation of the proximal coronary arteries. Taken together with these observations, it is suggested that three distinct cell types are involved in the formation of the proximal coronary artery, PEO-derived subepicardial mesenchymal cells, endothelial cells from the sinus venosus, and neural crest-derived pharyngeal mesenchymal cells.

In conclusion, our results suggest that TNC may play a role in the recruitment of smooth muscle cells to the nascent coronary artery.

Acknowledgements

The authors thank Prof. H Nakamura of Saitama Medical University for permitting us to use the TRI/3D-SRF-II system and Ms. S Uoya and M Namikata for providing technical assistance. This work was supported by JSPS grants-in-Aid for Scientific Research #20390052, 21659047 (YN), 20590174(KA), 2059310(SMT) and 21590927(KIY).

Appendix A. supplementary materials

Supplementary data associated with this article can be found in the online version at doi:10.1016/j.diff.2011.03.002.

References

Ando, K., Nakajima, Y., Yamagishi, T., Yamamoto, S., Nakamura, H., 2004. Development of proximal coronary arteries in quail embryonic heart: multiple capillaries penetrating the aortic sinus fuse to form main coronary trunk. Circ. Res. 94, 346–352.

Ballard, V.L.T., Sharma, A., Duignan, I., Holm, J.M., Chin, A., Choi, R., Hajjar, K.A., Wong, S.-C., Edelberg, J.M., 2006. Vascular tenascin-c regulates cardiac endothelial phenotype and neovascularization. FASEB J. 20, 717–719.

Bogers, A.J.J.C., Gittenberger-de, Groot, A.C., Poelmann, R.E., Péault, B.M., Huysmans, H.A., 1989. Development of the origin of the coronary arteries, a matter of ingrowth or outgrowth? Anat. Embryol. 180, 437–441.

Castellon, R., Caballero, S., Hamdi, H.K., Atilano, S.R., Aoki, A.M., Tarnuzzer, R.W., Kenney, M.C., Grant, M.B., Ljubimov, A.V., 2002. Effects of tenascin-C on normaland diabetic retinal endothelial cells in culture. Invest. Ophthalmol. Vis. Sci. 43, 2758–2766.

Compton, L.A., Potash, D.A., Mundell, N.A., Barnett, J.V., 2006. Transforming growth factor-*β* induces loss of epithelial character and smooth muscle cell differentiation in epicardial cells. Dev. Dyn. 235, 82–93.

Crossin, K.L., Hoffman, S., 1991. Expression of adhesion molecules during the formation and differentiation of the avian endocardial cushion tissue. Dev. Biol. 145, 277–286.

Gurevicius, K., Kuang, F., Stoenica, L., Irintchev, A., Gureviciene, I., Dityatev, A., Schachner, M., Tanila, H., 2009. Genetic ablation of tenascin-C expression leads to abnormal hippocampal CA1 structure and electrical activity in vivo. Hippocampus 19, 1232–1246.

Hamburger, V., Hamilton, H.L., 1992. A series of normal stages in the development of the chick embryo. Dev. Dyn. 195, 231–272.

Hellström, M., Kalén, M., Lindahl, P., Abramsson, A., Betsholtz, C., 1999. Role of PDGF-B and PDGFR-beta in recruitment of vascular smooth muscle cells and pericytes during embryonic blood vessel formation in the mouse. Development 126, 3047–3055.

Hirakow, R., 1983. Development of the cardiac blood vessels in staged human embryos. Acta. Anat 115, 220–230.

Hiruma, T., Hirakow, R., 1989. Epicardial formation in embryonic chick heart: computer-aided reconstruction, scanning, and transmission electron microscopic studies. Am. J. Anat. 184, 129–138.

Hurle, J.M., Garcia-Martinez, V., Ros, M.A., 1990. Immunofluorescent localization of tenascin during the morphogenesis of the outflow tract of the chick embryo heart. Anat. Embryol. 181, 149–155.

Imanaka-Yoshida, K., Hiroe, M., Nishikawa, T., Ishiyama, S., Shimojo, T., Ohta, Y., Sakakura, T., Yoshida, T., 2001a. Tenascin-C modulates adhesion of cardiomyocytes to extracellular matrix during tissue remodeling after myocardial infarction. Lab. Invest. 81, 1015–1024.

Imanaka-Yoshida, K., Matsuura, R., Isaka, N., Nakano, T., Sakakura, T., Yoshida, T., 2001b. Serial extracellular matrix changes in neointimal lesions of human coronary artery after percutaneous transluminal coronary angioplasty: clinical significance of early tenascin-C expression. Virchows. Arch. 439, 185–190.

Imanaka-Yoshida, K., Matsumoto, K., Hara, M., Sakakura, T., Yoshida, T., 2003. The dynamic expression of tenascin-C and tenascin-X during early heart development in the mouse. Differentiation 71, 291–298.

Imanaka-Yoshida, K., Hiroe, M., Yoshida, T., 2004. Interaction between cell and extracellular matrix in heart disease: multiple roles of tenascin-C in tissue remodeling. Histol. Histopathol. 19, 517–525.

Ishii, K., Imanaka-Yoshida, K., Yoshida, T., Sugimura, Y., 2008. Role of stromal tenascin-C in mouse prostatic development and epithelial cell differentiation. Dev. Biol. 324, 310–319.

Ishii, Y., Langberg, J., Rosborough, K., Mikawa, T., 2009. Endothelial cell lineages of the heart. Cell Tissue Res. 335, 67–73.

Ishigaki, T., Imanaka-Yoshida, K., Shimojo, N., Matsushima, S., Taki, W., Yoshida, T.. Tenascin-C enhances crosstalk signaling of integrin *αvβ*3/PDGFR-*β* complex by SRC recruitment promoting PDGF-induced proliferation and migration in smooth muscle cells. J. Cell Physiol.. (Epub ahead).

Jallo, G.I., Friedlander, D.R., Kelly, P.J., Wisoff, J.H., Grumet, M., Zagzag, D., 1997. Tenascin-C expression in the cyst wall and fluid of human brain tumors correlates with angiogenesis. Neurosurgery 41, 1052–1059.

Jiang, X., Rowitch, D.H., Soriano, P., McMahon, A.P., Sucov, H.M., 2000. Fate of the mammalian cardiac neural crest. Development 127, 1607–1616.

Jones, F.S., Jones, P.L., 2000. The tenascin family of ECM glycoproteins: Structure, function, and regulation during embryonic development and tissue remodeling. Dev. Dyn. 218, 235–259.

Kataoka, H., Takakura, N., Nishikawa, S., Tsuchida, K., Kodama, H., Kunisada, T., Risau, W., Kita, T., Nishikawa, S.I., 1997. Expressions of PDGF receptor alpha, c-Kit and Flk1 genes clustering in mouse chromosome 5 define distinct subsets of nascent mesodermal cells. Dev. Growth Differ 39, 729–740.

Kattan, J., Dettman, R.W., Bristow, J., 2004. Formation and remodeling of the coronary vascular bed in the embryonic avian heart. Dev. Dyn. 230, 34–43.

Landerholm, T.E., Dong, X.R., Lu, J., Belaguli, N.S., Schwartz, R.J., Majesky, M.W., 1999. A role for serum response factor in coronary smooth muscle differentiation from proepicardial cells. Development 126, 2053–2062.

Männer, J., 1999. Does the subepicardial mesenchyme contribute myocardioblasts to the myocardium of the chick embryo heart? A quail-chick chimera study tracing the fate of the epicardial primordium. Anat. Rec. 255, 212–226.

Matsui, H., Sakabe, M., Sakata, H., Yanagawa, N., Ikeda, K., Yamagishi, T., Nakajima, Y., 2008. Induction of initial heart -actin, smooth muscle -αctin, in chick pregastrula epiblast: The role of hypoblast and fibroblast growth factor-8. Dev. Growth. Differ. 50, 143–157.

Mellgren, A.M., Smith, C.L., Olsen, G.S., Eskiocak, B., Zhou, B., Kazi, M.N., Ruiz, F.R., Pu, W.T., Tallquist, M.D., 2008. Platelet-derived growth factor receptor β signaling is required for efficient epicardial cell migration and development of two distinct coronary vascular smooth muscle Cell populations. Circ. Res. 103, 1393–1401.

Metzger, R.J., Klein, O.D., Martin, G.R., Krasnow, M.A., 2008. The branching programme of mouse lung development. Nature 453, 733–735.

Midwood, K.S., Orend, G., 2009. The role of tenascin-C in tissue injury and tumorigenesis. J. Cell Commun. Signal 3, 287–310.

Mikawa, T., Gourdie, R.G., 1996. Pericardial mesoderm generates a population of coronary smooth muscle cells migrating into the heart along with ingrowth of the epicardial organ. Dev. Biol. 174, 221–232.

Mu, H., Ohashi, R., Lin, P., Yao, Q., Chen, C., 2005. Cellular and molecular mechanisms of coronary vessel development. Vasc. Med. 10, 37–44.

Nahirney, P.C., Mikawa, T., Fischman, D.A., 2003. Evidence for an extracellular matrix bridge guiding proepicardial cell migration to the myocardium of chick embryos. Dev. Dyn. 227, 511–523.

Nishioka, T., Onishi, K., Shimojo, N., Nagano, Y., Matsusaka, H., Ikeuchi, M., Ide, T., Tsutsui, H., Hiroe, M., Yoshida, T., Imanaka-Yoshida, K., 2010. Tenascin-C may aggravate left ventricular remodeling and function after myocardial infarction in mice. Am. J. Physiol. Heart Circ. Physiol. 298, H1072–H1078.

Olivey, H.E., Compton, L.A., Barnett, J.V., 2004. Coronary vessel development: the epicardium delivers. Trends. Cardiovasc. Med. 14, 247–251.

Paik, D.C., Fu, C., Bhattacharya, J., Tilson, M.D., 2004. Ongoing angiogenesis in blood vessels of the abdominal aortic aneurysm. Exp. Mol. Med. 36, 524–533.

Poelmann, R.E., Gittenberger-de, Groot, A.C., Mentink, M.M., Bokenkamp, R., Hogers, B., 1993. Development of the cardiac coronary vascular endothelium, studied with antiendothelial antibodies, in chicken-quail chimeras. Circ. Res. 73, 559–568.

Ratajska, A., Czarnowska, E., Ciszek, B., 2008. Embryonic development of the proepicardium and coronary vessels. Int. J. Dev. Biol. 52, 229–236.

Red-Horse, K., Ueno, H., Weissman, I.L., Krasnow, M.A., 2010. Coronary arteries form by developmental reprogramming of venous cells. Nature 464, 549–553.

Reese, D.E., Mikawa, T., Bader, D.M., 2002. Development of the coronary vessel system. Circ. Res. 91, 761–768.
Saga, Y., Yagi, T., Ikawa, Y., Sakakura, T., Aizawa, S., 1992. Mice develop normally without tenascin. Genes Dev. 6, 1821–1831.
Tamaoki, M., Imanaka-Yoshida, K., Yokoyama, K., Nishioka, T., Inada, H., Hiroe, M., Sakakura, T., Yoshida, T., 2005. Tenascin-C regulates recruitment of myofibroblasts during tissue repair after myocardial injury. Am. J. Pathol. 167, 71–80.
Tanaka, K., Hiraiwa, N., Hashimoto, H., Yamazaki, Y., Kusakabe, M., 2004. Tenascin-C regulates angiogenesis in tumor through the regulation of vascular endothelial growth factor expression. Int. J. Cancer 108, 31–40.
Tucker, R.P., Chiquet-Ehrismann, R., 2009. The regulation of tenascin expression by tissue microenvironments. Biochim. Biophys. Acta 1793, 888–892.
Sugi, Y., Markwald, R.R., 1996. Formation and early morphogenesis of endocardial endothelial precursor cells and the role of endoderm. Dev. Biol. 175, 66–83.
Van Den Akker, N.M.S., Lie-Venema, H., Maas, S., Eralp, I., DeRuiter, M.C., Poelmann, R.E., Gittenberger-De, Groot, A.C., 2005. Platelet-derived growth factors in the developing avian heart and maturating coronary vasculature. Dev. Dyn. 233, 1579–1588.
Waldo, K.L., Willner, W., Kirby, M.L., 1990. Origin of the proximal coronary artery stems and a review of ventricular vascularization in the chick embryo. Am. J. Anat. 188, 109–120.
Verzi, M.P., McCulley, D.J., De Val, S., Dodou, E., Black, B.L., 2005. The right ventricle, outflow tract, and ventricular septum comprise a restricted expression domain within the secondary/anterior heart field. Dev. Biol. 287, 134–145.
Vrancken Peeters, M.-P.F.M., Gittenberger-de, Groot, A.C., Mentink, M.M.T., Hungerford, J.E., Little, C.D., Poelmann, R.E., 1997. The development of the coronary vessels and their differentiation into arteries and veins in the embryonic quail heart. Dev. Dyn. 208, 338–348.
Zagzag, D., Shiff, B., Jallo, G.I., Greco, M.A., Blanco, C., Cohen, H., Hukin, J., Allen, J.C., Fridlander, D.R., 2002. Tenascin-C promotes microvascular cell migration and phosphorylation of focal adhesion kinase. Cancer Res. 62, 2660–2668.
Zhang, H.Y., Kluge, M., Timpl, R., Chu, M.L., Ekblom, P., 2006. The extracellular matrix glycoproteins BM-90 and tenascin are expressed in the mesenchyme at sites of endothelial-mesenchymal conversion in the embryonic mouse heart. Differentiation 52, 211–220.

Supplemental Table 1

TNC (μg/ml)	Number of cells migrated
0 (n=14)	104±27
2 (n=14)	94±25
5 (n=9)	97±32

Transwell migration assay: The epicardia from ED6 chick hearts were prepared on cell culture insert (8-μm pore size, Becton Dickinson Labware) as described in materials and methods. The medium containing 2% chick serum was poured into the outer chamber (Falcon 24-well plate, Becton Dickinson Labware). To examine the effect of TNC on cell migration, purified TNC (0-5μg/ml) was added to serum-free medium of the upper chamber. The cells from the epicardium were allowed to migrate to the lower membrane surface for 48 h. The epicardial cells on the upper surface were wiped off and the inserts were fixed with 100% ethanol and stained with Coomassie Brilliant Blue. Stained cells on the lower membrane surface were counted under a ×20 objective lens (total cells/epicardial explant). Statistical analysis was performed using the unpaired *t*-test, and the significance was set at <5%. The results showed that there was no significant difference in the number of cells that migrated across the membrane between the control and TNC-rich cultures. n, number ofexplant examined.

Effects of transforming growth factor-β3 and matrix metalloproteinase-3 on the pathogenesis of chronic mitral valvular disease in dogs

Koji Obayashi, DVM; Sachiko Miyagawa-Tomita, DVM, PhD; Hirotaka Matsumoto, DVM, PhD; Hidekazu Koyama, DVM, PhD; Toshio Nakanishi, MD, PhD; Hisashi Hirose, DVM, PhD

Objective—To investigate the roles of transforming growth factor-β (TGF-β) isoforms and matrix metalloproteinases (MMPs) in development of chronic mitral valvular disease (CMVD) in dogs.

Sample Population—12 mitral valve leaflets collected from cadavers of 5 clinically normal dogs and from 7 dogs with CMVD.

Procedures—Expression of TGF-β isoforms 1, 2, and 3; MMPs 1, 2, 3, and 9; TGF-β receptor II (TβR-II); and α smooth muscle actin (αSMA) in mitral valves of dogs with CMVD was compared with that in mitral valves from clinically normal dogs. Additionally, responses of valvular interstitial cells (VICs) to TGF-β3, MMP-3, and angiotensin-converting enzyme inhibitor (ACEI) as a suppressor of TGF-β3 were examined in vitro.

Results—Expression of TGF-β3, TβR-II, αSMA, and MMP-3 was only detected in mitral valves of dogs with CMVD. Concentrations of αSMA and proteoglycans in cultured VICs were significantly increased following incubation with TGF-β3; treatment with MMP-3 resulted in increased amounts of active and total TGF-β3, and total TGF-β3 in VICs was significantly decreased by incubation with ACEI.

Conclusions and Clinical Relevance—Findings suggested that increased TGF-β3 and MMP-3 contribute to the pathogenesis of valvular degeneration associated with CMVD. In addition, it is possible that the use of ACEI could effectively block pathological alterations in VICs associated with CMVD in vitro.

Impact on Human Medicine—CMVD is associated with primary mitral valve prolapse and Marfan syndrome in humans. Results of the study reported here will help to elucidate the molecular mechanisms of CMVD in dogs and humans. (*Am J Vet Res* 2011;72:194–202).

Chronic mitral valvular disease, also known as myxomatous mitral valve disease, is one of the most commonly acquired cardiovascular diseases in geriatric dogs and is a major cause of morbidity and early death in this species.[1,2] The pathophysiologic changes associated with CMVD cause the mitral valve leaflets to become abnormally thickened, and subsequent malfunction of the mitral valve results in mitral regurgitation. This disease is caused by valvular degeneration and is also characterized by disruption of the collagen and elastin matrix architecture and accumulation of proteoglycans in the spongiosa.[3–5]

The causes and molecular mechanisms of these pathological processes are unknown. However, mechanical stress[6] to the valvular endothelium, VICs, or both has been proposed to lead to pathological transformation of VICs and also to the release of mediators that affect production of proteoglycans and reduction

Abbreviations

ACEI	Angiotensin-converting enzyme inhibitor
αSMA	α Smooth muscle actin
CMVD	Chronic mitral valvular disease
ECM	Extracellular matrix
MMP	Matrix metalloproteinase
p-SMAD2	Phosphorylated Sma and Mad protein 2
TβR-I	Transforming growth factor β receptor I
TβR-I ALK5	Transforming growth factor β receptor I activin receptor-like kinase 5
TβR-II	Transforming growth factor β receptor II
TGF-β	Transforming growth factor β
VIC	Valvular interstitial cell

Received September 3, 2009.
Accepted December 8, 2009.
From the Department of Veterinary Internal Medicine, Faculty of Veterinary Medicine, Nippon Veterinary and Life Science University, 1-7-1 Kyonan-cho, Musashino-shi, Tokyo 180-8602, Japan (Obayashi, Matsumoto, Koyama, Hirose); the Department of Pediatric Cardiology, Heart Institute, Tokyo Women's Medical University, 8-1 Kawada-cho, Shinjuku-ku, Tokyo 162-8666, Japan (Obayashi, Miyagawa-Tomita, Nakanishi); and the Division of Cardiovascular Development and Differentiation, Medical Research Institute, Tokyo Women's Medical University (Miyagawa-Tomita).
Dr. Miyagawa-Tomita was supported in part by Grant-in-Aid for Scientific Research (C).
The authors thank Dr. Koji Tanizawa for providing materials.
Address correspondence to Dr. Miyagawa-Tomita (ptomita@hij.twmu.ac.jp).

of collagen. Several reports[6–10] have suggested that a pathological alteration in VICs is necessary for the development of valvular degeneration. Endothelin,[11–13] nitric oxide,[14] MMPs[6,9,15] and TGF-β isoforms[16] are among the proposed potential mediators; however, the precise contribution of these and other potential mediators of valvular degeneration remains unclear.

Chronic mitral valvular disease in dogs is similar to mitral valve prolapse and to the valvular diseases associated with Marfan syndrome in humans. Studies of mice with phenotypes of mitral valve prolapse[17] and with features of Marfan syndrome[18] strongly suggested that enhanced MMP-2 or TGF-β signaling may be related to the pathogenesis of mitral valve prolapse.

Members of the MMP family of zinc-dependent endoproteases play important roles in ECM degradation in many tissues, including cardiac valves.[19] The TGF-β family of ligands and receptors includes TGF-β, bone morphogenetic proteins, activins, and inhibins. Three major isoforms of TGF-β, designated TGF-β1, TGF-β2, and TGF-β3, are produced in multiple cell types and participate in a wide array of cellular responses including proliferation, differentiation, inflammation, ECM deposition, and apotosis.[20] The TGF-β isoforms are synthesized as prepropolypeptides that are proteolytically processed in the Golgi apparatus to a mature growth factor and its propeptide, also known as latency-associated peptide. Dimers of mature TGF-β and latency-associated peptide form a tight complex, termed the small latency complex, which is biologically inactive. The small latency complex is covalently bound to another protein called latent TGF-β binding protein, forming a large latency complex. The large latency complex is secreted from cells to the extracellular space, where it binds to the ECM. Several inducers of TGF-β activation have been proposed, including proteolytic enzymes (such as MMPs), the matricellular protein thrombospondin-1, integrins, and ionizing radiation.[20–24]

Although some reports have suggested that TGF-β and MMPs are related to valvular degeneration,[6,9,16,18,25] to the authors' knowledge, no study has shown how these factors affect progression of valvular degeneration. Furthermore, although ACEI has been used well in clinical settings, the effect of ACEI on valvular degeneration has not been reported. The study reported here was performed to investigate the roles that TGF-β isoforms and MMPs play in the development of CMVD in dogs and to provide further insight into the pathogenesis of CMVD.

Materials and Methods

Animals and tissue collection—Hearts were collected from 12 dogs that died naturally or were euthanized. Each dog had previously undergone a physical examination by a veterinarian at the Hospital for Small Animals at Nippon Veterinary and Life Science University or at a referring clinic. Three dogs underwent radiography, 7 underwent radiography and echocardiography, and 2 underwent neither of these procedures. Cardiothoracic ratio,[26] vertebral heart size,[27] and left atrial-to-aortic root ratio[28] were measured as part of the thoracic radiographic and echocardiographic examinations. Seven of the 12 dogs (various breeds; 2 males and 5 females; median age, 11.7 years) each had a clinical diagnosis of CMVD, and these were classified as the CMVD group. Dogs with CMVD had been treated with benazepril hydrochloride, benazepril hydrochloride plus furosemide, or a combination of these drugs with digoxin until the time of death. Because these dogs were client owned, consent for use of tissues in the study was obtained from owners prior to necropsy. Hearts were removed from the dogs (which died naturally despite medical treatment during hospitalization) within 1 hour of death. The 5 remaining dogs were clinically normal Beagles (2 males and 3 females; median age, 3.8 years) that were used for educational purposes in the veterinary teaching hospital. These dogs were not receiving any medications and were classified as the clinically normal group. These dogs were euthanized for reasons not related to the present study via IV administration of thiopental sodium, and hearts were collected within 30 minutes of death. The study was approved by the Bioethics Committee at Nippon Veterinary and Life Science University.

Gross pathologic and histologic examination—The presence or absence of CMVD was confirmed on gross examination and independently classified according to Whitney criteria,[16,29] as subjectively determined by 2 investigators (KO and HH). Valves and chordae tendineae were considered normal when they had thin translucent leaflets with no nodular thickening. Classification of mild CMVD was determined when valves met the criteria for Whitney type I or II classifications (type I changes were characterized by a few small, discrete areas of opacity or nodules in the area of valvular apposition, and type II changes comprised a subjectively increased number of larger nodules) but the chordae tendineae were not affected. Valves of dogs with moderate CMVD met the criteria for Whitney type III classification; these contained either large nodules or plaque-like deformities, and thickening of the chordae tendineae was detected visually. Valves of dogs considered to have severe CMVD met the criteria for Whitney type IV classification; the valves were contracted and distorted, and the free edges of the leaflets may thus have rolled toward the left atrium. The proximal aspect of the chordae tendineae was thickened, elongated, and sometimes ruptured in dogs with severe CMVD.

Following gross examination, half of the anterior mitral valve leaflets were used for culture of VICs, and the heart with remaining leaflets was fixed in 4% formalin for 24 hours at 25°C. Five-micrometer-thick longitudinal tissue sections were dewaxed in xylene and rehydrated through a graded series of ethanol. Some sections were stained with H&E, Masson trichrome stain, Victoria blue-van Gieson stain, and Alcian blue stain.

Antibodies were obtained from various sources, and all antibodies were diluted in blocking solution (PBSS supplemented with 10% normal goat serum). Some sections were pretreated with PBSS supplemented with 0.3% hydrogen peroxide to inhibit endogenous peroxidase activity, incubated in blocking solution, and then incubated with primary antibodies (each diluted 1:400) at 4°C overnight, which included mouse anti-porcine vimentin[a]; rabbit anti-chicken desmin[b]; rabbit anti-human TGF-β1,[c] TGF-β2,[c] TGF-β3,[c] TβR-II,[d]

TβR-I ALK5,[c] MMP-1,[e] and MMP-3[e]; and goat anti-human MMP-2[c] and MMP-9.[c] Sections were also incubated with mouse anti-human αSMA[f] (diluted 1:1,000). Secondary antibodies (biotinylated anti-mouse IgG,[g] anti-rabbit IgG,[g] or anti-goat IgG[g] [each diluted 1:200]) were applied to the sections for 30 minutes at 25°C according to the source of primary antibodies. Immunoreactivities were detected by use of a peroxidase-labeled avidin-biotin complex kit,[h] and peroxidase activity was detected by use of 3,3′-diaminobenzidine tetrahydrochloride[i] as a chromagen substrate. Sections were counterstained with hematoxylin. To create negative control tissue sections, the primary antibody was replaced with mouse IgG,[g] rabbit IgG,[j] or goat IgG.[k] For positive control tissues, chick embryonic and canine heart sections (obtained in our laboratory from unrelated experiments) were used.

Culture and immunostaining of VICs—For in vitro culture of VICs,[30] anterior mitral valve leaflets collected from the 5 clinically normal dogs were excised one-third of the distance from the base of the cusp. The leaflets were washed in PBSS on ice and then minced into small pieces. The pieces (1 to 2 mm^2) were plated and cultured (37°C, 5% CO_2, and 100% humidity) in Iscove modified Dulbecco medium[l] supplemented with 10% fetal bovine serum[m] and 1% antibiotic-antimycotic.[l] According to the method of Pho et al,[30] collected cells were split 1:3 at 70% confluence and the cells from passages 3 to 5 were used to seed cultures for each experiment. Primary antibodies against TGF-β1, TGF-β2, TGF-β3, TβR-II, MMP-3, αSMA, desmin, vimentin (all diluted as described for tissue sections), and mouse anti-human CD31[n] (diluted 1:200) were used to test cultured cells. The latter 3 antibodies were used as markers of myocardial, mesenchymal, and endothelial cells, respectively.

The VICs were seeded at 5×10^3 cells/cm^2 and were maintained in complete culture medium as previously described (the day of seeding was considered day 0). After 3 days and at approximately 70% confluence, the cells were immunostained[30] in culture plates. The cells were rinsed once with PBSS and fixed for 10 minutes in 4% paraformaldehyde in PBSS at 25°C. Cells were permeabilized with PBSS supplemented with 0.1% nonionic surfactant solution,[o] incubated with blocking solution for 1 hour, and then incubated with primary antibodies at 4°C overnight. The cells were incubated with the previously described biotinylated secondary antibodies for 30 minutes at 25°C and then incubated with fluorescence-labeled streptavidin solution.[p] Nuclei were counterstained with 4',6'-diamidino-2-phenylindole. Cells were examined and images were obtained by use of a fluorescence microscope,[q] and the number of cells that were positive for desmin, vimentin, and αSMA were counted; percentages of the total cell count were calculated by dividing the number of positively labeled cells by the number of 4',6'-diamidino-2-phenylindole–stained cells.

Western blotting—After seeding as described (day 0), cultured VICs were incubated for 3 days with the following treatments in separate wells: goat anti-chicken TGF-β3 neutralizing antibody[r] (5 μg/mL), TGF-β3 peptide[s] (1 ng/mL or 10 ng/mL), or TGF-β3 peptide (1 ng/mL) plus [3-(Pyridin-2-yl)-4-(4-quinonyl)]-1H-pyrazole (a 5μM TβR-I kinase inhibitor).[t] Cultured VICs with no treatment were used as control samples. After 3 days of incubation, cultured VICs were lysed in lysis buffer solution[u] and centrifuged at 12,000 × *g* at 4°C for 15 minutes, and the supernatant was recovered. Protein concentration was measured by use of a protein assay kit,[v] and equal amounts of total protein were separated via SDS-PAGE with 12% Bis-tris–containing polyacrylamide gels[l] and then transferred to polyvinylidene difluoride membranes. The membranes were incubated with the previously described anti-αSMA (diluted 1:1,000), rabbit anti-human p-SMAD2[w] (1:500), and mouse anti-human β actin[e] antibodies (1:2,000), followed by AP-conjugated anti-mouse IgG or anti-rabbit IgG secondary antibodies[x] selected according to the source of the primary antibodies. Blots were developed by use of a chemiluminescent detection system,[x] and bands were detected by use of an image analysis system.[y] The bands were quantified by use of an optional software application supplied with the image analyzer.[y]

Proteoglycans analysis—Proteoglycans were quantified by use of a commercially available mu-

Table 1—Characteristics of 7 dogs with CMVD.

Age (y)	Breed	Sex	Medication	CR (%)	VHS (No. of vertebral lengths)	LA: Ao	Cause of death	Whitney type
14	Pomeranian	F	BNZ, furosemide, digoxin	72.7	12.1	ND	PE	IV
12	Maltese	M	BNZ, furosemide, digoxin	ND	ND	ND	PE	IV
12	Miniature Dachshund	F	BNZ, furosemide, digoxin	77.4	10.4	ND	PE	IV
13	Shi Tzu	F	BNZ, furosemide, digoxin	73.4	11.5	ND	PE	IV
11	Shi Tzu	F	BNZ, furosemide, digoxin	ND	ND	ND	PE	IV
10	Beagle	F	BNZ	67.0	10.4	1.54	Pn	III
10	Beagle	M	BNZ, furosemide	69.0	13.0	1.87	PE	IV

All dogs had previously undergone physical examination; 3 dogs had also undergone only radiography, 2 had undergone radiography and echocardiography, and 2 had undergone neither of these procedures. The cause of death was respiratory insufficiency related to heart failure with pulmonary edema or pneumonia. During postmortem gross examination, mitral valves were evaluated according to Whitney criteria[16,29]; dogs were considered to have moderate or severe CMVD when valves met criteria for Whitney type III or IV classfications, respectively. None of the mitral valves met criteria for Whitney type I or II classifications (ie, mild CMVD).

BNZ = Benazepril hydrochloride. CR = Cardiothoracic ratio. F = Female. LA:Ao = Left-atrial-to-aortic-root ratio. M = Male. ND = Not determined. PE = Pulmonary edema. Pn = Pneumonia. VHS = Vertebral heart size.

copolysaccharide assay kit.[z] The assay was performed according to the manufacturer's instructions. The same treatments were applied to cultured VICs as described for western blot analysis. The VICs were lysed in lysis buffer at 60°C for 1 hour; lysates were combined with reaction buffer, and absorbance at 650 nm was measured via a spectrophotometer.

ELISAs—An ELISA specific for the active human TGF-β3 homodimer[aa] was used to assess the amount of TGF-β3 in VICs incubated with MMP-3, MMP-3 plus an MMP-3 inhibitor, ACEI, or no treatment (as controls) in separate experiments. Cultured cell suspensions were treated according to the manufacturer's instructions; samples were acidified by addition of 1N HCl. After 10 minutes, the sample was neutralized with 1.2N NaOH (to determine the total amount of TGF-β3). Active TGF-β3 was measured in samples prior to acid treatment.

For all ELISAs, microplates were coated with anti–TGF-β3 capture antibody overnight at 25°C and blocked with PBSS supplemented with 1% bovine serum albumin for 1 hour. Samples or standards were added to coated plates, incubated at 25°C for 2 hours, and then aspirated. Each plate was incubated with anti–TGF-β3 detection antibody for 2 hours, followed by incubation with horseradish peroxidase–conjugated streptavidin solution. Color development was achieved by addition of the substrate, and the reaction was allowed to proceed for 20 minutes. When color development was complete, the reaction was stopped by the addition of 2N H_2SO_4 and absorbance at 450 nm was measured via a spectrophotometer.

To assess the effect of MMP-3 on amounts of active and total TGF-β3 in cultured cell suspension (which included VICs and ECM), VICs were treated with recombinant human MMP-3[bb] (30 ng/mL; activated before use via incubation with 4-aminophenylmercuric acetate[f] at 37°C for 20 hours) or with the MMP-3 treatment combined with 4-(4′-Biphenyl)-4-hydroxyiminobutyric acid MMP-3 inhibitor[cc] at 37°C for 1 hour.

To assess the effect of ACEI on TGF-β3 synthesis in VICs, the VICs were incubated with an ACEI[dd] (2mM) for 3 days. The total TGF-β3 concentration in the cell suspension was measured.

Statistical analysis—Results are expressed as the mean ± SD for 3 independent experiments. A statistical analysis was performed by use of a 2-tailed Mann-Whitney *U* test or by use of ANOVA with a Student-Newman-Keuls test. Results were considered to be statistically significant for values

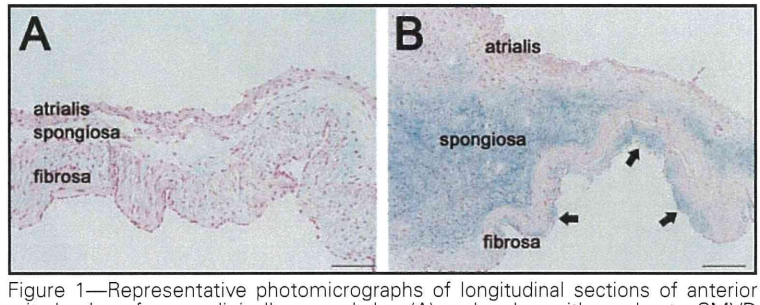

Figure 1—Representative photomicrographs of longitudinal sections of anterior mitral valves from a clinically normal dog (A) and a dog with moderate CMVD (B). In panel A, the normal mitral valve has 3 well-defined tissue layers: atrialis, spongiosa, and fibrosa. In panel B, the mitral valve from a dog with CMVD has an abnormally layered architecture with an expanded spongiosa strongly positive for proteoglycans (blue), loose collagen and accumulation of proteoglycans (arrows) in the fibrosa, and disrupted elastin in the atrialis. The distal aspect of the valve leaflet is on the left. The proximal aspect of the valve leaflet is on the right. Alcian blue stain; the bar in panel A represents 100 μm, and the bar in panel B represents 200 μm.

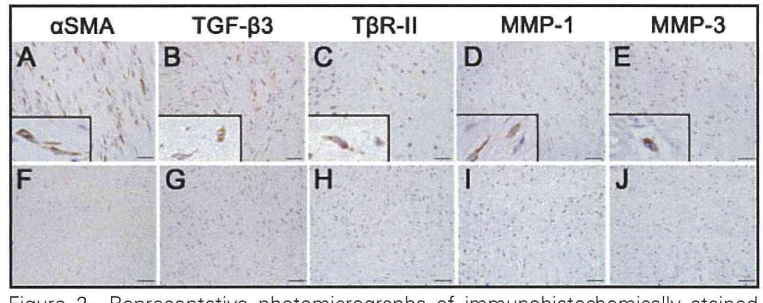

Figure 2—Representative photomicrographs of immunohistochemically stained sections of anterior mitral valves from dogs with CMVD (panels A through E) and from clinically normal dogs (F through J). Expression of αSMA (panels A and F), TGF-β3 (B and G), TβR-II (C and H), and MMP-3 (E and J) was detected in VICs of all dogs with CMVD, but was not detected in those of dogs without CMVD. Expression of MMP-1 was detected in VICs of 3 of 7 dogs with CMVD (panel D), but was not detected in those of clinically normal dogs (I). Positive expression is indicated by brown labeling of cells. Sections were counterstained with hematoxylin. Bars = 50 μm; inset (lower left) of panels in the top row, 600X magnification.

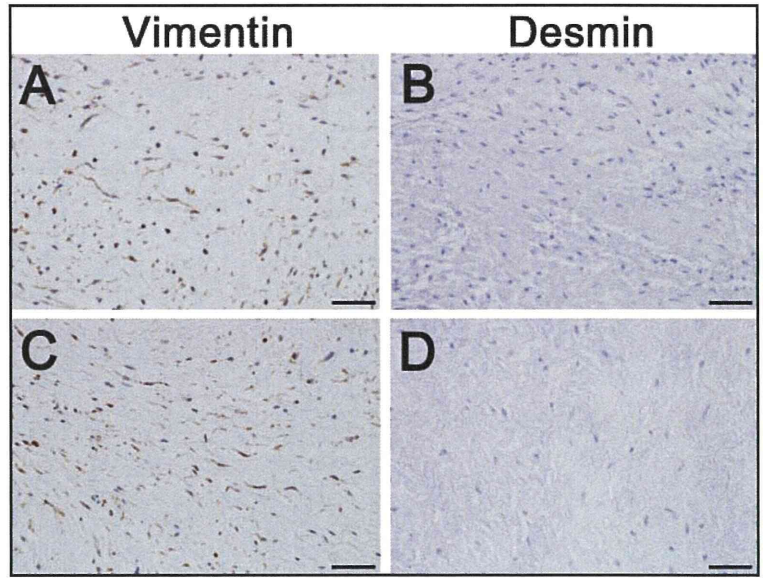

Figure 3—Representative photomicrographs of immunohistochemically stained sections of anterior mitral valves from dogs with CMVD (panels A and B) and from clinically normal dogs (C and D). In mitral valves of dogs of both groups, cytoplasmic expression of vimentin (A and C) but not desmin (B and D) was detected in VICs. *See* Figure 2 for remainder of key.

of $P \leq 0.05$. All analyses were performed by use of a commercially available statistical software program.[ee]

Results

Clinical findings and gross morphology of the heart—The mitral valves of the 5 clinically normal dogs were all classified as normal during gross pathological examination. The 7 dogs with CMVD each had a left systolic regurgitant heart murmur of grade 3/6 or higher. Echocardiographic findings of mitral regurgitation (including irregular and thickened mitral valve leaflets) were assessed in 2 dogs with CMVD. Radiographic findings included enlargement of the heart in 5 dogs with CMVD (increased cardiothoracic ratio [mean value, 71.9%; normal ratio, ≤ 65%[26]] and vertebral heart size [mean value, 11.48 vertebral lengths; normal value, 9.7 ± 0.5 vertebral lengths[27]). Cause of death (determined on the basis of physical examination and necropsy findings, which included radiographic analysis for 5/7 dogs, results of a CBC for 2/7 dogs, and results of serum biochemical analysis for 1/7 dogs) was respiratory insufficiency related to heart failure with pulmonary edema or pneumonia. Of the 7 dogs in the CMVD group, gross examination of the hearts revealed that 1 had moderate CMVD and 6 had severe CMVD (**Table 1**).

Histopathology and immunohistochemistry—Histologic findings for anterior mitral valves from clinically normal dogs were compared with those from dogs in the CMVD group (**Figure 1**). The 3 tissue layers of the valves (the atrialis, mainly composed of elastic fibers and few collagen fibers; the centrally located spongiosa, composed of small amounts of proteoglycans; and the fibrosa, predominantly composed of collagen fibers arranged parallel to the free edge of the leaflet) were well-defined in clinically normal dogs, and the surface of these valves was covered by a single layer of endothelial cells. In contrast, anterior mitral valves from dogs in the CMVD group were characterized by multifocal expansion of the valvular layers, predominantly due to increased deposition of proteoglycans in the spongiosa.

In anterior mitral valves of all dogs with CMVD, intracytoplasmic expression of αSMA, TGF-β3, and TβR-II was detected in VICs in the deep regions of the atrialis and spongiosa layers; in contrast, VICs in the valves of clinically normal dogs did not have detectable expression of these factors (**Figure 2**). The VICs in mitral valves of dogs in both groups expressed vimentin, TGF-β1, and TGF-β2 in the cytoplasm and TβR-I ALK5 in the cytoplasm and nucleus, but did not express detectable amounts of desmin (**Figures 3 and 4**).

The VICs in anterior mitral valves from 7 of 7 dogs with CMVD expressed MMP-3 in the cytoplasm, and in 3 of 7 dogs with CMVD, these cells also expressed MMP-1 in the cytoplasm (Figure 2). However, no expression of MMP-2 or MMP-9 was detected in mitral valve VICs of dogs with CMVD (**Figure 5**). No positive expression of MMP-1, MMP-2, MMP-3, or MMP-9 was detected in VICs of mitral valves from clinically normal dogs.

Immunocytochemistry of cultured mitral valve VICs—Cultured VICs from clinically normal dogs were

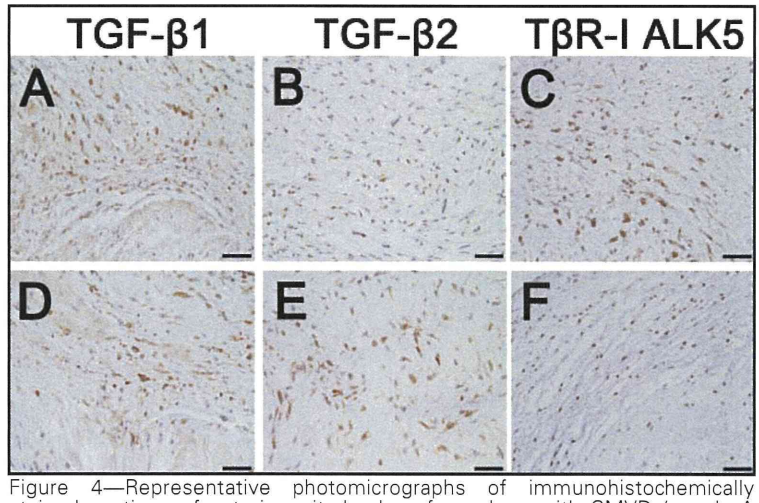

Figure 4—Representative photomicrographs of immunohistochemically stained sections of anterior mitral valves from dogs with CMVD (panels A through C) and from clinically normal dogs (D through F). The mitral valve VICs of dogs of both groups expressed TGF-β1 and TGF-β2 in the cytoplasm and expressed TβR-I ALK5 in cytoplasm and nuclei; TGF-β1 (indicated by light brown labeling) was also expressed in ECM in the spongiosa layer (panels A and D). *See* Figure 2 for key.

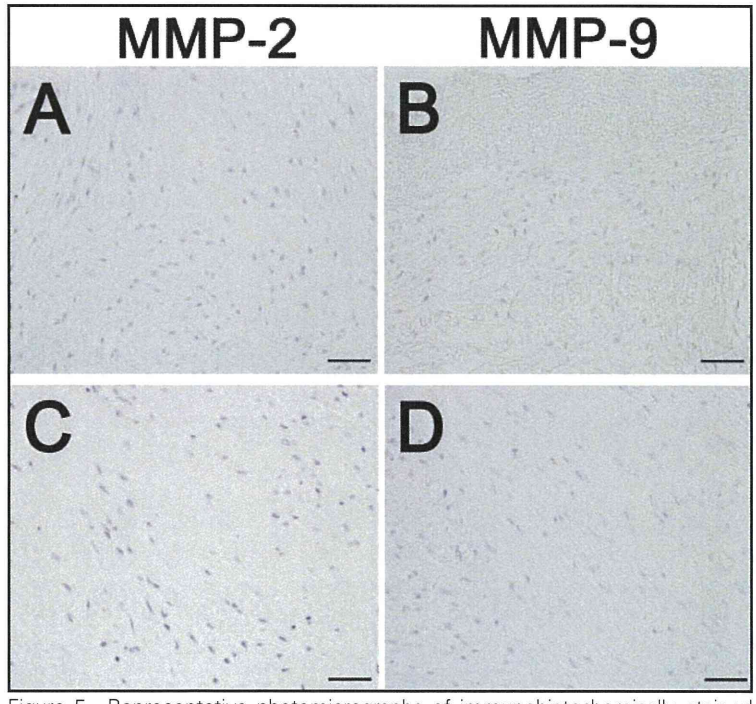

Figure 5—Representative photomicrographs of immunohistochemically stained sections of anterior mitral valves from dogs with CMVD (panels A and B) and from clinically normal dogs (C and D). Expression of MMP-2 or MMP-9 was not detected in the mitral valve VICs of dogs of either group. *See* Figure 2 for key.

confirmed to include no endothelial cells by use of antibodies against the adhesion molecule CD31, and only a small number of cells (≤ 1%) tested positive for the myocardial cell marker desmin (data not shown). The cultured VICs had a spindle-shaped phenotype, and approximately 65% of the cells expressed detectable amounts of αSMA (**Figure 6**). More than 95% of VICs also tested positive for the expression of vimentin (data not shown). The VICs expressed TGF-β2, TGF-β3, TβR-II, and MMP-3 but did not express detectable amounts of TGF-β1. The immunoreactivity patterns in cultured VICs were similar to those detected during histologic analysis of VICs in mitral valves from dogs with CMVD.

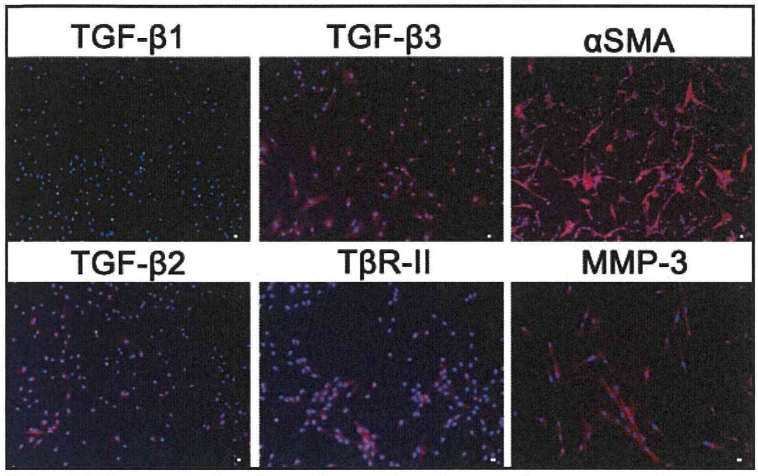

Figure 6—Representative photomicrographs of immunofluorescence detection in VICs cultured from the mitral valves of clinically normal dogs. The VICs expressed TGF-β3, αSMA, TGF-β2, TβR-II, and MMP-3; expression of TGF-β1 was not detected. The immunoreactive patterns detected in cultured VICs resemble those detected in the mitral valve VICs of CMVD-affected dogs via immunohistochemical analysis. Positive result is indicated by red fluorescence; nuclei are counterstained with 4', 6'-diamidino-2-phenylindole (blue fluorescence). Bars = 200 μm.

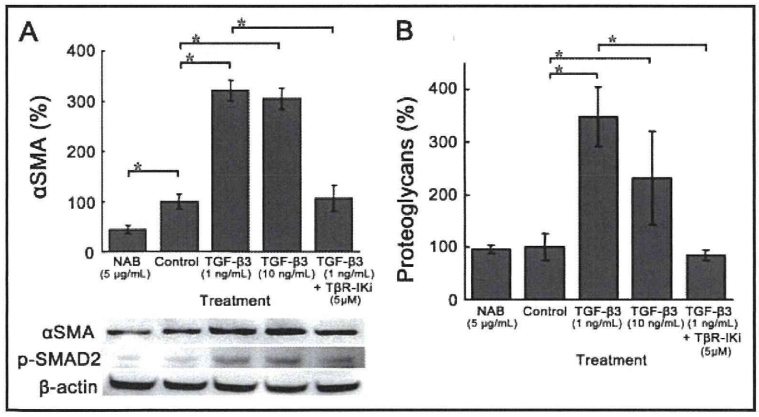

Figure 7—Results of analysis of TGF-β3 activation or inhibition in cultured VICs of clinically normal dogs. Cultured cells were treated with TGF-β3 neutralizing antibody (NAB), no treatment (control), TGF-β3, or TGF-β3 plus TβR-I kinase inhibitor (TβR-IKi). In panel A, western blots of cultured cell lysates were probed with antibodies against αSMA, p-SMAD2, and β-actin; the graph indicates mean ± SD concentrations of αSMA protein normalized to β-actin of the control sample, and photographs of representative blots are displayed. Concentrations of αSMA were significantly decreased by treatment with NAB and were significantly increased by treatment with TGF-β3; this response was significantly inhibited by the addition of TβR-IKi. In panel B, analysis of proteoglycans concentration in lysates of cultured VICs was performed by use of a mucopolysaccaride assay kit. The graph indicates mean ± SD concentrations of proteoglycans relative to the amount of total protein in the control sample. Treatment with TGF-β3 caused a significant increase in VIC proteoglycan synthesis, which was significantly inhibited by the addition of TβR-IKi. *$P < 0.01$.

TGF-β3 activation of cultured VICs and inhibition of TGF-β3—The VICs that were incubated for 3 days with a neutralizing antibody known to recognize the TGF-β3 isoform had significantly ($P < 0.01$) decreased expression of αSMA (mean ± SD, 44 ± 7%; **Figure 7**). Conversely, stimulation with TGF-β3 induced a significant increase in αSMA expression in cultured VICs; the results of analysis of western blots indicated that αSMA expression increased significantly ($P < 0.01$) after treatment with TGF-β3 at concentrations of 1 ng/mL (321 ± 21%) or 10 ng/mL (305 ± 21%) and that this increase was significantly ($P < 0.01$) blocked by treatment with TβR-I kinase inhibitor (106 ± 26%). Expression of p-SMAD2 was increased but was nonsignificant after TGF-β3 treatment. The morphology of VICs was not changed by the culture system or by the described treatments.

Effect of TGF-β3 on proteoglycans synthesis—The addition of TGF-β3 (1 or 10 ng/mL) to VICs in culture for 3 days resulted in significantly ($P < 0.01$) increased synthesis of proteoglycans (348 ± 56% and 231 ± 89%, respectively). Treatment with TβR-I kinase inhibitor significantly ($P < 0.01$) suppressed the effect of TGF-β3 on proteoglycans synthesis (84 ± 10%; Figure 7).

MMP-3 mediated changes in amounts of active and total TGF-β3—The ability of MMP-3 to trigger the release of active and total TGF-β3 from cultured VICs was confirmed via ELISA (**Figure 8**). Treatment with recombinant human MMP-3 caused significant ($P < 0.05$ and $P < 0.01$, respectively) increases in the mean ± SD concentrations of active (untreated control cells, 9.6 ± 4.0 pg/mL; MMP-3 treated cells, 21.3 ± 5.4 pg/mL) and total (untreated control cells, 24.4 ± 7.1 pg/mL; MMP-3 treated cells, 52.9 ± 4.1 pg/mL) TGF-β3 from the cultured VIC layer. Thereafter, the reactions were significantly ($P < 0.05$) inhibited via addition of the MMP-3 inhibitor (mean ± SD concentrations of active and total TGF-β3, 8.3 ± 3.8 pg/mL and 36.0 ± 6.7 pg/mL, respectively). Treatment with 1 ng/mL TGF-β3 had no influence on the total amount of MMP-3 expression from VICs (data not shown).

Effect of ACEI on TGF-β3 expression—The effect of ACEI on TGF-β3 synthesis in VICs was also assessed via ELISA (Figure 8). Treatment with ACEI caused a significant ($P < 0.05$) decrease in the mean ± SD concentrations of total TGF-β3 in cultured VICs (untreated control cells, 33.4 ± 1.5 pg/mL; ACEI-treated cells, 20.3 ± 1.8 pg/mL).

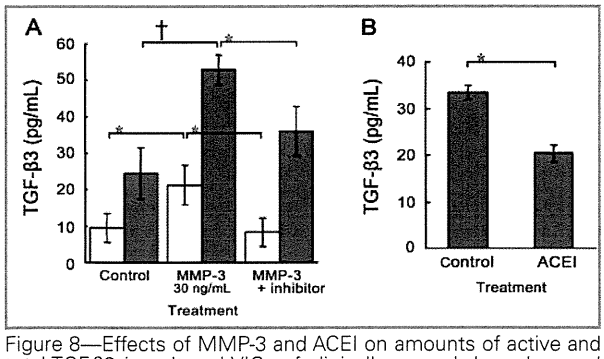

Figure 8—Effects of MMP-3 and ACEI on amounts of active and total TGF-β3 in cultured VICs of clinically normal dogs. In panel A, mean ± SD concentrations of active (white bars) and total (gray bars) TGF-β3 in cultured cells were quantified via ELISA. To determine amounts of active and total TGF-β3, ELISAs were performed before and after acid activation with 1N HCl, respectively. Amounts of active and total TGF-β3 in cultured cells were significantly increased by treatment with recombinant human MMP-3, compared with that of untreated (control) samples; this increase was suppressed by the addition of an MMP-3 inhibitor. In panel B, the total concentration of TGF-β3 in cultured cells was determined via ELISA. Values were significantly decreased by treatment with ACEI, compared with concentrations in control samples. *$P < 0.05$. †$P < 0.01$.

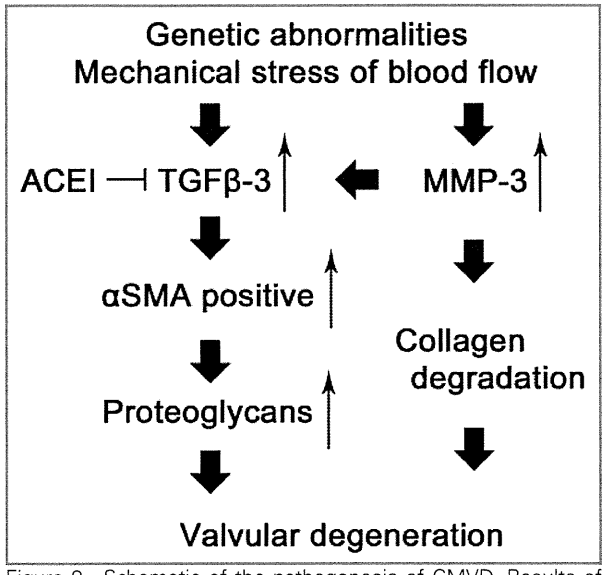

Figure 9—Schematic of the pathogenesis of CMVD. Results of the present study suggested that increased concentrations of TGF-β3 and MMP-3 contribute to the pathogenesis of CMVD and that ACEI may suppress TGF-β3–induced mechanisms of pathogenesis. Thin arrows indicate upregulation. Perpendicular intersecting lines indicate suppression.

Pathogenesis of CMVD—Results of the MMP-3, TGF-β3, and ACEI experiments were used to develop a schematic of the pathogenesis of CMVD in dogs (Figure 9). This model incorporated the effects of MMP-3 on TGF-β3 expression and the potential contributions of these factors to the valvular degeneration process.

Discussion

The study reported here demonstrated the roles of TGF-β3 and MMP-3 in the pathogenesis of CMVD in dogs and revealed relationships among TGF-β3, MMP-3, and activated VICs. Nonactivated VICs in healthy cardiac valves have a fibroblast-like morphology, and these cells synthesize collagen, elastin, and proteoglycans. In valves affected by CMVD, degeneration has been mainly detected in the spongiosa layer,[31] and previous reports[6–10] have suggested that phenotypically altered VICs were found in diseased mitral valves; the αSMA-positive cells were characterized as myofibroblasts. In the present study, αSMA positive cells (which are myofibroblasts) were only detected in valves from dogs with CMVD. Therefore, myofibroblasts are considered to play an important role in the pathogenesis of valvular degeneration.

Aupperle et al[16] described the expression patterns of TGF-β isoforms in mitral valves from healthy dogs and from dogs with CMVD, but expression patterns detected in the study reported here were not identical to those findings. The results of the Aupperle et al[16] study indicated increased expression of TGF-β1 and TGF-β3 and weak expression of TGF-β2 in diseased valves. In the present study, however, expression of TGF-β3 and of TβR-II was only detected in the mitral valves of dogs with CMVD, and TGF-β1 and TGF-β2 were equally expressed in mitral valves of clinically normal dogs and dogs with CMVD. These differences may have been attributable to the use of antibodies obtained from different manufacturers, to different fixation times, or to the immunohistochemistry methods that were used.

Although other studies[16,18] indicated that TGF-β1 might play an important role in mitral valve degeneration, results of the present study indicated that mitral valves of clinically normal dogs and of dogs with CMVD equally expressed TGF-β1, whereas TGF-β3 was only expressed in diseased valves. We hypothesized that TGF-β3 and TGF-β1 might cause mitral valvular degeneration in a coordinated manner or that TGF-β3, together with factors other than TGF-β1, might induce this disease. Therefore, we focused particularly on the role of TGF-β3. Little is known about the specific function of TGF-β3; however, TGF-β1, TGF-β2, and TGF-β3 may have distinct functions in the epithelial-mesenchymal transformation that occurs during cardiac valve development.[32] Transforming growth factor-β3 regulates the quality and quantity of ECM and also has a crucial role in atrioventricular valve remodeling in avian species.[33] In the present study, we demonstrated that TGF-β3 singularly regulated valve myofibroblast activation and proteoglycan synthesis in an in vitro system. The modulation attributed to TGF-β3 at least partially involved the p-SMAD2 signaling pathway. The reactions of cultured VICs may not be identical to processes that occur in VICs in vivo because cultured VICs undergo selection processes and stress caused by conditions of the culture itself. In addition, the expression of αSMA has been reported[34] to vary somewhat, depending on the culture period of VICs. A report[6] has also shown that abnormalities of TGF-β3 signaling caused by genetic mutations or mechanical stress may promote pathological ECM remodeling in mitral valves.

The results of some studies[9,15] have also suggested that MMP-1, MMP-2, MMP-13, and MMP-14, as well as tissue inhibitors of metalloproteinase 2 and 3, were expressed in grossly and histologically normal mitral valves of dogs and were involved in ECM metabolism.

Increased expression of MMP-1, MMP-13, and MMP-14 was detected in mitral valves of dogs with CMVD in those studies. In humans, increased expression of MMP-1, MMP-2, MMP-9, and MMP-13 was confirmed in myxomatous heart valves, compared with expression in normal heart valves.[6,25] In the present study, MMP-1 and MMP-3 were only expressed in mitral valves of dogs with CMVD, and MMP-2 and MMP-9 were not expressed in mitral valves of dogs in either group. Expression of MMP-3 in cultured cells of various types was reported to be upregulated in vitro by means of mechanical stimulation, hydrostatic pressure,[35] or stretching.[36] Matrix metalloproteinase-3 degrades a wide range of substrates, including fibronectin; laminin; collagens III, IV, IX, X; and proteoglycans; it also activates pro-MMPs such as pro–MMP-1. It is possible that MMP-3 and MMP-1 may be involved in the destruction of the basal structure of mitral valves.

It is still unclear whether the abnormal accumulation of proteoglycans is a cause or a result of the degradation of ECM. However, the accumulation of proteoglycans may follow the degradation of ECM caused by MMPs.[25] Furthermore, analysis of the results of the study reported here indicated that MMP-3 also increased amounts of active and total TGF-β3. Therefore, MMP-3 and TGF-β3 might contribute to the accumulation of proteoglycans in this tissue.

Treatment with ACEIs has been useful in the management of hypertension and congestive heart disease in humans and dogs. Angiotensin II directly induces the transcription of *Tgfb1* in rats.[37] Analysis of results of the present study indicated that an ACEI effectively suppressed the amount of total TGF-β3 in vitro, which suggests that ACEIs may be useful for the prevention or treatment of CMVD; however, additional experiments should be performed to confirm that the reported effect was caused by prevention of angiotensin II formation in cultured VICs.

The study reported here was limited because the number of dogs was small and almost all of the dogs with a diagnosis of CMVD had clinically severe disease; we were unable to collect samples from dogs that had either mild or early stages of CMVD. We collected tissue specimens from privately owned dogs that had developed CMVD and died naturally. Since most owners cherished their dogs, it was extremely difficult for us to obtain permission to perform postmortem examinations. There were differences in the ages and breeds of dogs between the clinically normal and CMVD groups. The incidence of CMVD has been observed to increase with advancing age. Some studies[38–40] revealed that concentrations of TGF-β isoforms[38,39] and MMPs[40] in human plasma or serum also change with age; as age increased, concentrations of TGF-β1, TGF-β3, and MMP-9 decreased and concentrations of TGF-β2, MMP-2, and MMP-7 increased. Thus, it may be possible that the ages or breeds of the dogs may have affected expression patterns of proteins that were examined in the present study.

Our results indicate that increased TGF-β3 and MMP-3 protein concentrations in mitral valves contribute to the pathogenesis of CMVD in dogs. The factors that regulate TGF-β3 and MMP-3 are still unknown, although it is thought that this regulation involves genetic mechanisms and mechanical stress. Further research is needed to identify new markers for use in the diagnosis of this disease and for the development of new medicines that act on the molecular mechanisms of valvular degeneration.

a. AbD Serotec, Kidlington, Oxfordshire, England.
b. Progen, Land Baden-Württemberg, Germany.
c. Santa Cruz Biotechnology Inc, Santa Cruz, Calif.
d. Upstate Biotechnology, Billerica, Mass.
e. Abcam, Cambridge, England.
f. Sigma-Aldrich Corp, St Louis, Mo.
g. Vector Laboratories Inc, Burlingame, Calif.
h. ABC Elite kit, Vector Laboratories Inc, Burlingame, Calif.
i. Diaminobenzidine, Wako Pure Chemical Industries Ltd, Osaka, Japan.
j. Inter-Cell Technologies Inc, Hopewell, NJ.
k. Chemicon International Inc, Billerica, Mass.
l. Invitrogen Corp, Carlsbad, Calif.
m. Fetal bovine serum, Biowest, Paris, France.
n. DAKO, Glostrup, Denmark.
o. Triton X-100, Wako Pure Chemical Industries Ltd, Osaka, Japan.
p. Streptavidin Hilyte Plus 647 conjugated (60672-Plus647), AnaSpec, Gauteng, South Africa.
q. Fluorescence microscope BZ-8000, Keyence Corp, Osaka, Japan.
r. R&D Systems Inc, Minneapolis, Minn.
s. TGF-β3 peptide (PT-4124), Lonza Group Ltd, Basel-Stadt, Switzerland.
t. TβR-I kinase inhibitor, Calbiochem, Hesse, Germany.
u. CelLytic-M, Sigma-Aldrich Corp, St Louis, Mo.
v. DC protein assay kit, Bio-Rad Laboratories Inc, Hercules, Calif.
w. Signalway Antibody Inc, Pearland, Tex.
x. WesternBreeze chemiluminescent detection system, Invitrogen Corp, Carlsbad, Calif.
y. LAS-3000 UV mini image analysis system with optional software application Multi Gauge software program, version 3.0, FUJIFILM, Tokyo, Japan.
z. Acidic Mucopolysaccaride assay kit, Primary Cell, Hokkaido, Japan.
aa. Active human TGF-β3 homodimer DuoSet ELISA, R&D Systems Inc, Minneapolis, Minn.
bb. Recombinant human MMP-3, AnaspecAnaSpec, Gauteng, South Africa.
cc. MMP-3 Inhibitor VI, Calbiochem, Hesse, Germany.
dd. Enalapril maleate, Sigma-Aldrich Corp, St Louis, Mo.
ee. Ystat 2006, version 5, Igaku Tosho Shuppan, Tokyo, Japan.

References

1. Darke PG. Valvular incompetence in Cavalier King Charles Spaniels. *Vet Rec* 1987;120:365–366.
2. Beardow AW, Buchanan JW. Chronic mitral valve disease in Cavalier King Charles Spaniels: 95 cases (1987–1991). *J Am Vet Med Assoc* 1993;203:1023–1029.
3. Devereux RB. Recent developments in the diagnosis and management of mitral valve prolapse. *Curr Opin Cardiol* 1995;10:107–116.
4. Fontana ME, Sparks EA, Boudoulas H, et al. Mitral valve prolapse and the mitral valve prolapse syndrome. *Curr Probl Cardiol* 1991;16:309–375.
5. King BD, Clark MA, Baba N, et al. "Myxomatous" mitral valves: collagen dissolution as the primary defect. *Circulation* 1982;66:288–296.
6. Rabkin E, Aikawa M, Stone J, et al. Activated interstitial myofibroblasts express catabolic enzymes and mediate matrix remodeling in myxomatous heart valves. *Circulation* 2001;104:2525–2532.
7. Corcoran BM, Black A, Anderson H, et al. Identification of surface morphologic changes in the mitral valve leaflets and chordae tendineae of dogs with myxomatous degeneration. *Am J Vet Res* 2004;65:198–206.
8. Black A, French AT, Dukes-McEwan J, et al. Ultrastructural